Impact of Coal-Carrying Trains on Particulate Matter Concentrations in the Lower Mainland region of British Columbia, Canada

by

Kevin J. Akaoka

B.Sc. (Hons.), The University of Western Ontario, 2012

A THESIS SUBMITTED IN PARTIAL FULFILLMENT
OF THE REQUIREMENTS FOR THE DEGREE OF

Master of Science

in

The Faculty of Graduate and Postdoctoral Studies

(Atmospheric Science)

The University of British Columbia

(Vancouver)

October 2015

Abstract

The transport of coal by train through residential neighbourhoods in Metro Vancouver, British Columbia, Canada is a growing concern for many residents living near the railway. This study aimed to identify and quantify any potential particulate matter (PM) increase caused by the presence of rail traffic adjacent to John Oliver Park in Delta, BC.

Field work was carried out during August and September 2014, using a GRIMM optical particle counter that measured PM concentration at various size ranges. A select number of passing trains were confirmed visually, while the majority of passages were identified with audio data recorded by a microphone. A horizontally operating mini-micropulse lidar system was also set up at the park on three individual days to make intensive backscatter measurements. Wind data were recorded by collocated instruments maintained by Metro Vancouver. Finally, the Corporation of Delta had a dustfall measurement campaign during the same time period.

Trains carrying coal are associated with a 5.28, 4.11, and 2.55 μg/m^3 average increase in concentration over a 15 minute period, compared to control conditions for PM_3, PM_{10}, and PM_{20}, respectively. These increases are all statistically significant at $\alpha = 0.01$. PM concentrations during train passages of all types were not found to be significantly different from PM concentrations during control conditions. The presence of coal dust particles at the site was confirmed by the dustfall measurements carried out by the Corporation of Delta.

Lidar backscatter imagery provided individual snapshots of train passages. However, it is clear that not every train passage causes an increase in PM concentration, and the effect appears to be highly dependent on wind direction and local meteorology.

Preface

This thesis consists of original, unpublished, and independent work completed by the author. Input on research design and analysis was provided by Dr. Ian McKendry. All wind data and some PM concentration data used in Chapters 3 and 4 were provided by Metro Vancouver's Air Quality group. The dustfall observations in Section 3.4 were provided by the Corporation of Delta's Climate Action & Environment department. The lidar backscatter images in Chapter 4 were created by Paul Cottle.

Table of Contents

List of Tables

List of Figures

Acknowledgments

First and foremost, I would like to sincerely thank my mentor and thesis supervisor, Dr. Ian McKendry. This research project would not have been possible without his constant guidance, encouragement, and assistance. Moreover, I would like to thank the entire Department of Geography at UBC for adopting me and providing me with fantastic support for the entire duration of my graduate program.

Research funding was provided by Natural Sciences and Engineering Research Council (NSERC) operating grants to Dr. Ian McKendry. The author was financially supported by a scholarship from the NSERC Collaborative Research and Training Experience program in Atmospheric Aerosols (CREATE-AAP), in conjunction with top-up funds from the Department of Earth, Ocean, and Atmospheric Sciences at UBC.

There were numerous collaborators that were crucial in helping complete this research. I would like to personally thank: Dr. Julie Saxton and Ken Reid at Metro Vancouver, Stephanie Smith at Communities and Coal, Paul Cottle in the Department of Geography at UBC, Dr. Dan Jaffe at the University of Washington, and my field assistants Rachel Cliff, Meng Si, and Mark Richardson.

I am incredibly fortunate to have had a fantastic support system during my graduate studies. My colleagues and peers have inspired me countless times with their brilliance and dedication to their work. My friends and family, here in Vancouver and back home in Toronto have constantly supported me and made my transition into a new city and province so much easier. Finally, I would like to specially thank Mikayla Uber for her constant support, encouragement, and always being there for me.

Chapter 1

Introduction

1.1 Background

Exposure to particulate matter (PM) is a growing concern for residents of urban environments across the world. PM sources can be conceptualized as point sources (such as individual buildings), or they can be considered as 1-dimensional line sources. The most significant line sources for PM typically correspond to transportation corridors. There are numerous examples of studies focusing on PM concentrations along roadways, as well as the health effects one would experience living close to a roadway. However, little attention has been given to railways, where trains generate significant amounts of PM including diesel particulate matter (DPM) (Abbasi et al., 2013). DPM is characterized by fine and ultrafine particles of greatest concern to human health (Peters et al., 1997). Trains also contribute non-exhaust emissions related to the wearing down of train components, such as brake pads and wheels (Abbasi et al., 2013).

Even less work has been done regarding the generation of coal dust from freight trains. As trains with more than 100 open coal cars travel along railways to their destination, some of the coal dust may be lost into the air, affecting the local PM concentration (Jaffe et al., 2014). These particles are typically larger than DPM, allowing for their detection using size-segregated measuring techniques (Jaffe et al., 2014). The research described here is focused on the collection and analysis of PM concentrations measured adjacent to a railway running through the Lower Mainland region of British Columbia, Canada.

This railway is of particular interest, as previous work (Jaffe et al., 2014) has

studied emissions from coal-carrying trains at a different location along the same route, in the U.S. state of Washington. There is also concern from a public health perspective, as sections of the railway pass through densely populated neighbourhoods in White Rock, and Surrey, BC. Moreover, the future possibility of increased coal train traffic through the region suggests a need for research into the air quality impacts of coal trains.

1.2 Literature Review

1.2.1 Health Effects

Health impacts related to PM exposure have been well documented, with a general consensus in the air pollution epidemiology literature that both acute and ambient exposure to elevated PM concentrations results in detrimental health effects (Bascom et al., 1996; Dockery and Pope, 1994). These effects involve strain on the respiratory system, which over time may lead to the development of chronic respiratory diseases and increased mortality rates (Dockery and Pope, 1994). The damage suffered by the respiratory system is related to the size of the particles, with the smallest particles causing the highest level of respiratory distress (Peters et al., 1997). These particles in the fine mode of PM are typically referred to as $PM_{2.5}$, meaning all particles with diameters less than 2.5 μm. The second major category of particles is termed PM_{10}, or the coarse mode. In the context of the respiratory system, coarse particles typically impact and deposit in the upper respiratory tract (Heyder, 2004). Fine particles, in contrast, are able to travel further through the respiratory system, depositing in the lower respiratory tract, the portion of the system that includes the alveoli (Heyder, 2004). Given the sensitive nature of the alveoli, inflammation in this part of the system can lead to the most serious health effects (Peters et al., 1997).

1.2.2 Trains as a PM Source

For those living in urban environments, ambient PM exposure is typically associated with the transportation sector (Hoek et al., 2002). DPM has been the focus of several studies (e.g. Galvis et al. (2013); Liukonen et al. (2002); Zhu et al. (2002)) examining human exposure to PM caused by major transportation corridors (such

as freeways). In addition to motor vehicles, significant transportation-related emissions are from rail vehicles. Studies involving PM emissions from rail traffic divide the emissions into two broad source categories: exhaust and non-exhaust. "Non-exhaust" refers to sources such as the wearing down of rails, brake pads, and other similar railway components (Abbasi et al., 2013). Gehrig et al. (2007) concluded that PM_{10} concentrations at three Swiss railway sites with both freight and passenger traffic were indeed greater than those representative of a "background site". Further analysis indicated that the majority of the PM_{10} increase could be attributed to iron particles (Gehrig et al., 2007). Since trains in Switzerland are almost exclusively electric, only non-exhaust emissions were able to account for this increase. (Gehrig et al., 2007).

Exhaust emissions, specifically DPM, are of concern to human health due to the typically small size range of the particles generated. Liukonen et al. (2002) examined DPM by analyzing concentrations of elemental and organic carbon. The findings show a broad range of measured concentrations, likely dependent on several factors. Overall, the authors conclude that due to numerous confounding sources, elemental carbon concentrations are the best proxy for measuring DPM. Moreover, the exposure of train crews to DPM is "comparable to background urban exposures", with a range of <1 to 45 $\mu g/m^3$ being recorded.

1.2.3 Coal Dust

One aspect of this project's primary focus is on a specific non-exhaust emission source: coal dust from open train cars. Coal dust generation has been studied in both controlled conditions (e.g. Ferreira and Vaz (2004)), and, in recent years, real world conditions (e.g. Higginbotham et al. (2013) and Jaffe et al. (2014)). Ferreira and Vaz (2004) examined coal dust release from a scale model in a wind tunnel experiment. While the results of this study should not be expected to scale well to the real world, the authors demonstrated significant loss of mass at an undisturbed flow velocity of 13.4 m/s (Ferreira and Vaz, 2004). Interestingly, at a lower flow velocity (10.1 m/s), the coal particles were not lost from the scale model train cars, suggesting the presence of a threshold velocity required to initiate coal dust loss (Ferreira and Vaz, 2004).

Two studies conducted in 2013 directly examined PM increases related to the generation of coal dust and DPM from coal trains: Higginbotham et al. (2013) and

Jaffe et al. (2014). The former monitored a railway in Newcastle, Australia over three days, observing PM increases associated with the passage of 73 coal trains. Instruments were set up approximately 10 metres from the tracks, and measurements were segregated based on seven unique "signatures" representing variations in factors such as wind speed/direction and train speed (Higginbotham et al., 2013). All signatures showed a significant increase of PM_{10} concentration. The signatures from passing coal trains were also compared to a signature from a passing freight train carrying grain. This signature showed a smaller increase in PM concentration compared to the coal trains, suggesting that the coal train signature was due to coal dust deposition, rather than DPM (Higginbotham et al., 2013). Somewhat counter-intuitively, it appeared that unloaded coal trains exhibited a much larger signature than loaded trains (Higginbotham et al., 2013). However, the authors suggested that this could be the effect of train speed, as unloaded trains typically passed the site at higher speeds than loaded trains (Higginbotham et al., 2013). Moreover, size segegrated data (TSP, PM_{10}, $PM_{2.5}$, and PM_1) showed that the majority of the concentration increases were due to coarse mode particles, once again pointing to the effect of coal dust particles (Higginbotham et al., 2013).

Jaffe et al. (2014) conducted their study in and around Seattle, Washington with similar methodology to Higginbotham et al. (2013), while also including data on CO_2 concentration. This study collected PM concentration data at 10 second intervals using a DustTrak DRX Aerosol Monitor approximately 25 metres from the railway, detecting PM concentrations at the same size fractions as Higginbotham et al. (2013). The DustTrak DRX is a photometer, which operates similarly to the optical particle counter proposed for use in this project. The key conclusion from this paper is that on average, $PM_{2.5}$ concentrations increased by 6.8 $\mu g/m^3$ with the passing of a coal train (Jaffe et al., 2014). The data also showed that coal trains caused an increase in the concentrations of larger particles, which is theorized to be from aerosolized coal dust (Jaffe et al., 2014).

Another consideration discussed in Jaffe et al. (2014) and Higginbotham et al. (2013) is the effect of meteorology on PM measurements. Of greatest importance is the relationship between recorded PM concentrations and wind direction. If the instruments located at a study site are not downwind of the railway, measurements will underestimate any impact caused by passing trains. Jaffe et al. (2014) alleviated this problem by only analyzing events with a PM_1-CO_2 correlation coefficient of greater than 0.5, or an increase in CO_2 of more than 3 ppmv (parts per million of

volume). Additionally, the passing of a train travelling at high speed will disturb the air flow around it, further complicating these effects (Higginbotham et al., 2013).

1.2.4 Zone of Influence of a Linear Source

The health impacts of a given PM source are highly dependent on the zone of influence of the source. Much work has been done on determining the relationship between measured pollutant concentrations, and distance from a source. Karner et al. (2010) provides an excellent summary on the various studies attempting to identify a zone of influence for various pollutants, and the results show large amounts of variation. While each individual source is unique, differences are also caused by the pollutant being studied (Karner et al., 2010). For linear PM sources, the zone of influence is somewhat unclear. Some results show a minor or gradual decrease in concentration with distance, but there are other instances of PM concentration not having any relationship with distance (Karner et al., 2010; Roorda-Knape et al., 1998). For situations with a gradual decrease in PM concentration over distance, the background concentration was reached after 176 m, giving an idea of the potential size of a zone of influence (Karner et al., 2010).

1.3 Research Objectives

This study aims to build on previous work on emissions from coal trains by focusing on a few key areas of interest. As this research has implications in a variety of fields (i.e. meteorology, air pollution, and public health), the associated research objectives reflect this. They are as follows:

1. Investigate the impacts of coal-carrying trains on PM concentrations within 50 metres of the tracks. Specific goals include quantification of the magnitude, frequency, and duration of PM impacts. In addition, impacts of coal-carrying trains will be compared with other train types.

2. Utilize size-segregated PM measurements to determine the size distribution of PM emissions from coal trains.

3. Investigate the "zone of influence" of train PM sources by using concentrations measured at two distances from the track, and by using a novel horizontal deployment of a micropulse lidar system.

4. Explore the relationship between meteorological conditions and observed PM concentrations.

These research questions will be explored using data from a variety of sources. Chapter 3 focuses on a broad statistical analysis of observed PM concentration data, stratified by train type, as well as wind direction. The results from this analysis are then contrasted in Chapter 4 with a case study analysis of three intensive observation days, including data from a micropulse lidar system.

Chapter 2

Study Area and Methodology

2.1 Study Area

The Lower Mainland is an area with 2.5 million residents centred on the Fraser River (Statistics Canada, 2014). The city of Vancouver serves as the region's largest city. The Lower Mainland's coastal location makes it home to several important ports, all of which are overseen by Port Metro Vancouver, a federal agency. Port Metro Vancouver is Canada's largest port by tonnage, and the 4th largest in North America (Port Metro Vancouver, 2014). Westshore Terminals, located in Delta, BC, is Canada's largest coal exporting facility, exporting both metallurgical (used for the production of steel) and thermal (used for power generation) coal from mines in Alberta, British Columbia, Montana, and Wyoming (Westshore Terminals Ltd, 2014). Coal arrives at Westshore Terminals via trains operated by Canadian National Railway (CN), Canadian Pacific Railway (CP), and the BNSF Railway (Cascadia Discovery Institute, 2011).

BNSF trains entering Canada from the United States operate on a railway running adjacent to the Peace Arch border crossing in White Rock, BC. From here, the line follows the shore of Boundary Bay passing directly through downtown White Rock and Crescent Beach, a community northwest of White Rock. The railway then crosses both the Nicomekl and Serpentine Rivers as well as BC Highway 99, before arriving at Colebrook junction. At this junction, BNSF trains join westbound CP and CN traffic, with all traffic travelling through Delta and finally terminating at Westshore Terminals (Cascadia Discovery Institute, 2011).

The bulk of observations made for this study were taken at John Oliver Park, a

public park and sports facility in the southeastern corner of Delta, BC. The railway being studied passes directly by the southern edge of the park. This section of track is located west of Colebrook junction, and therefore, includes train traffic operated by all three of CN, CP, and BNSF. Rail traffic passing by John Oliver Park consists of trains carrying either mixed-freight, or coal, allowing for a direct comparison between these two types of traffic. Figure 2.1 shows an overview of the Lower Mainland with all of these locations labelled.

Figure 2.1: Map of Lower Mainland region of British Columbia, with relevant locations highlighted. Taken from Apple Maps Version 2.0. Map data from TomTom and others. Satellite data from DigitalGlobe.

In addition, there is a major freeway approximately 200 metres south of where the GRIMM was located. This freeway, British Columbia Highway 99 is a major north-south route connecting the communities of Richmond, Delta, and White Rock with both the United States border, and Vancouver. Traffic patterns follow a strongly commuter-influenced pattern: northbound traffic peaks in the morning rush hour, while southbound traffic peaks in the afternoon rush hour. The freeway therefore serves as a significant line source that runs parallel to the study railway.

2.1.1 Data Sources

The data collected at John Oliver Park can be broadly divided into three groups: wind data, PM data, and lidar data. In addition, some data were obtained via a collaboration with the Corporation of Delta, and Metro Vancouver, who were simultaneously conducting a study regarding PM impacts of coal trains. Detailed information on each of the data sources is shown in Table 2.1.

The various instruments used for this study were setup at three locations within the park (Figure 2.2). Location A is closest to the study railway, located approximately 15 m to the north. Location B is situated slightly further away, at 50 m from the study railway. Finally, Location C, where the lidar was utilized, was 400 m north of the study railway.

Table 2.1: Summary of data sources.

Operator	Location	Instrument	Variables Measured	Dates Measured
UBC	B	GRIMM OPC	PM concentration	12/08/2014 - 21/09/2014
UBC	C	SigmaSpace Mini-MPL	Backscatter and depolarization ratios	12/08/2014 - 21/09/2014
Metro Vancouver	A	E-Sampler Anemometer	PM concentration Wind speed/direction	12/08/2014 - 21/09/2014
Metro Vancouver	B	E-Sampler Anemometer	PM concentration Wind speed/direction	12/08/2014 - 21/09/2014
Corporation of Delta	A	Dustfall gauge	PM mass	04/01/2014 - 04/30/2014

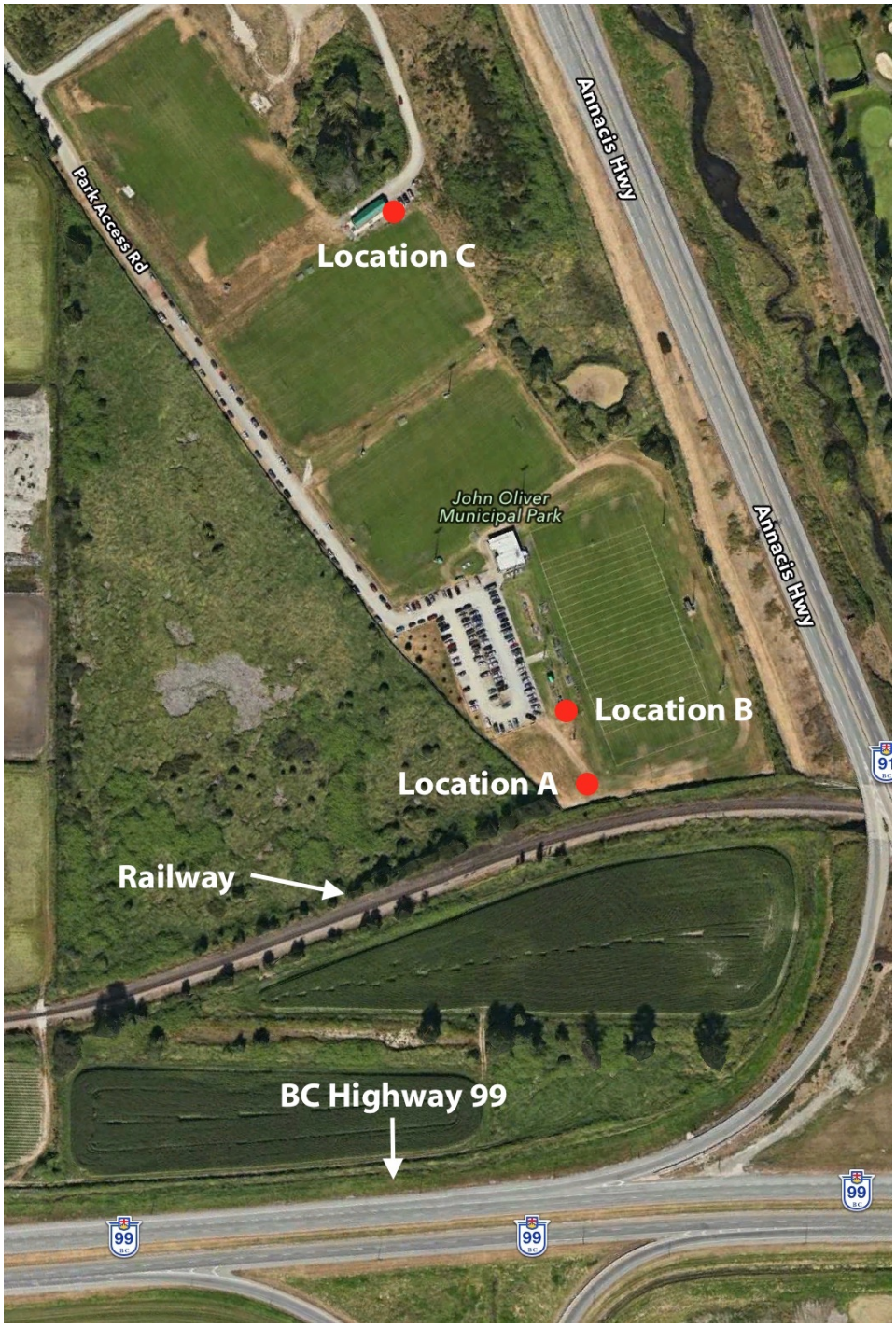

Figure 2.2: Map of John Oliver Park with instrument locations, taken from Apple Maps Version 2.0. Map data from TomTom and others. Satellite data from DigitalGlobe.

2.1.2 Instrumentation

PM concentration data were collected by UBC using a GRIMM 1.108 optical particle counter, and by Metro Vancouver using a Met One Instruments E-Sampler. The GRIMM 1.108 is a scattering-based instrument that measures particle counts at 16 different size bins, ranging from 0.23 to 20 μm. These particle counts can be used to indirectly calculate particle mass, and thus, particle concentrations. The determination of particle concentrations, is dependent on a gravimetric correction factor, which in turn is dependent on "particle density, shape, and refractive index" (GRIMM Aerosol Technik GmbH & Co. KG, 2010). A given site can be assumed to have a uniform particle density associated with its emissions (Maletto et al., 2003), meaning one calibration factor should be suitable for all measurements made at the same location.

The GRIMM OPC was housed in a Stevenson screen to protect it from precipitation and other external disturbances (Figure 2.3). The sample air was drawn into the instrument through a Teflon tube that was fed into the Stevenson screen. The usage of the GRIMM in this set up may affect the measurements in several different ways. Firstly, any bends in the Teflon tubing may result in impaction of particles on onto the sides of the tube (von der Weiden et al., 2009). The length of the tube may also prevent some particles larger than 0.5μm from reaching the instrument due to sedimentation processes within the tube (von der Weiden et al., 2009). Finally, as the GRIMM is a scattering-based instrument, the determination of particle size from scattering measurements is dependent on certain optical variables (GRIMM Aerosol Technik GmbH & Co. KG, 2010). The GRIMM was calibrated with dolomite dust, a material with different optical properties than coal dust, for example. Peters et al. (2006) compared the performance of the GRIMM to an aerodynamic particle sizer (APS), an instrument that is not dependent on optical properties. Both instruments measured a sample consisting of Arizona road dust, and the study concluded that the GRIMM "provided similar results to those from the APS" (Peters et al., 2006). The temporal resolution of measurements made using the GRIMM was initially set at 1 minute from 12/08/2014 to 26/08/2014. The remainder of the GRIMM measurements (from 26/08/2014 to 21/09/2014) were recorded at a 6 second resolution.

Lidar data were obtained using a SigmaSpace mini-micropulse lidar (mini-MPL), a relatively small, eye-safe remote sensing instrument capable of determining spatially and temporally averaged backscatter and depolarization ratios. The averaging time and distance was set to 30 seconds and 15 metres, respectively. The lidar oper-

Figure 2.3: Image of equipment set up location B. GRIMM OPC and Metro Vancouver E-Sampler and wind instrumentation shown.

ated with a laser energy of 3-4 μJ at 2500 hz, with a wavelength of 532 nm, appearing as green light. The instrument was mounted horizontally, and aimed at a heading of approximately 190°, which intersected the study railway at a nearly perpendicular angle. In addition, the mini-MPL requires at least 150 metres of distance before producing reliable data. Due to this, the mini-MPL was set up approximately 400 metres from the study railway (Figure 2.4).

The E-Sampler instrument used by Metro Vancouver uses a scattering-based approach similar to the GRIMM OPC, while also including gravimetric analysis to determine PM concentration. Data collected by Metro Vancouver includes concentrations of PM_{10} and $PM_{2.5}$. Two E-Samplers were employed by Metro Vancouver, yielding data at both 15 and 50 m from the study railway. In addition, wind direction and speed were recorded by Metro Vancouver using anemometers collocated with the E-Samplers. All data collected by Metro Vancouver was recorded at a temporal resolution of 1 minute.

The Corporation of Delta's dustfall measurements used a standardized "test

Figure 2.4: Image of mini-MPL set up at location C.

method for collection and measurement of dustfall" outlined by the standards organization ASTM International (Corporation of Delta, 2015).

2.1.3 Data Validation

The primary method of validating the GRIMM data was by comparison to data collected by Metro Vancouver. This data from the E-Sampler that was collocated with the GRIMM OPC was used to determine if the GRIMM was properly recording PM concentrations. The first comparison between data sets was done at a resolution of 1 minute. As the E-Sampler recorded PM_{10} concentrations, these values had to be calculated using the GRIMM data. The GRIMM reports concentrations in terms of concentrations of particles *larger* than each size cut. Thus, in order to estimate PM_{10} concentrations, the concentration for particles larger than 10.0 μm was subtracted from the concentration for particles larger than 0.23 μm (the smallest size cut).

Next, all values were averaged to a 1 minute resolution, to match the E-Sampler data.

At some periods during the study, the GRIMM may have been impacted by adverse weather conditions that included significant rainfall, leading to moisture accumulating within the intake tube. As such, there are several instances of the GRIMM recording concentrations that are highly suspect and unreasonable given the nature of the study site. These periods are characterized by sustained concentration values larger than 150 μg/m^3, or simply, concentration values of 0 μg/m^3. Any unreliable data that was qualitatively identified as such was therefore removed from the data set. A list of these periods is shown in Table 2.2.

Table 2.2: Description of periods of unreliable particle concentration data recorded by the GRIMM OPC.

Dates/Times
2014-08-13 09:26 - 10:00
2014-08-14 02:29 - 03:04
2014-08-14 05:27 - 05:42
2014-08-24 23:49 - **2014-09-02** 23:59
2014-09-11 23:18 - 23:20
2014-09-14 16:55 - 18:50
2014-09-15 19:45 - 20:05
2014-09-19 23:20 - **2014-09-21** 07:32

This reduced data set was then directly compared to the E-Sampler data. As seen in Figure 2.5, the GRIMM data appears to have more variability, with more extreme values than the E-Sampler data. Nevertheless, the large-scale trends over the span of several days do seem to match between the data sets. The scatterplot in Figure 2.6 confirms this, as the GRIMM data has numerous high concentration values associated with low values recorded by the E-Sampler. Overall, there is some weak correlation between the data sets (r = 0.177). One method used to filter out some of the extreme values recorded by the instruments was to use a 99th percentile cutoff to remove the top percent of values from the data. This results in a stronger correlation coefficient of 0.353.

Given the nature of the study location, and the difference in instruments, the data sets were also compared after being averaged to 30 minute time steps. This

strategy once again serves to filter out extreme variability, at the expense of filtering out any short-term spikes in PM_{10} concentration, such as those potentially associated with train passages. Nevertheless, this strategy was useful in comparing data sets and validating the GRIMM data.

At a 30 minute resolution, there is a much stronger relationship between the two data sets. Visually, it can be seen that concentration variations on a roughly diurnal scale are captured by both instruments in a very similar way (Figure 2.7). It is important to note that the GRIMM appears to record lower concentrations than the E-Sampler, with the exception of various periodic spikes (Figure 2.7). The potential sources of particle loss caused by the Teflon tubing used by the GRIMM (discussed in Section 2.1.2) may help explain the lower concentration values. The scatterplot in Figure 2.8 shows a much tighter distribution, and a moderate correlation coefficient of 0.552.

If both of these strategies (using a 99th percentile cut-off, and averaging to 30 minutes) are employed, the agreement between the two data sets is quite strong. Figure 2.9 shows that both diurnal-scale variations and the short-term spikes coincide as well. The correlation coefficient in this instance is once again higher, at 0.646.

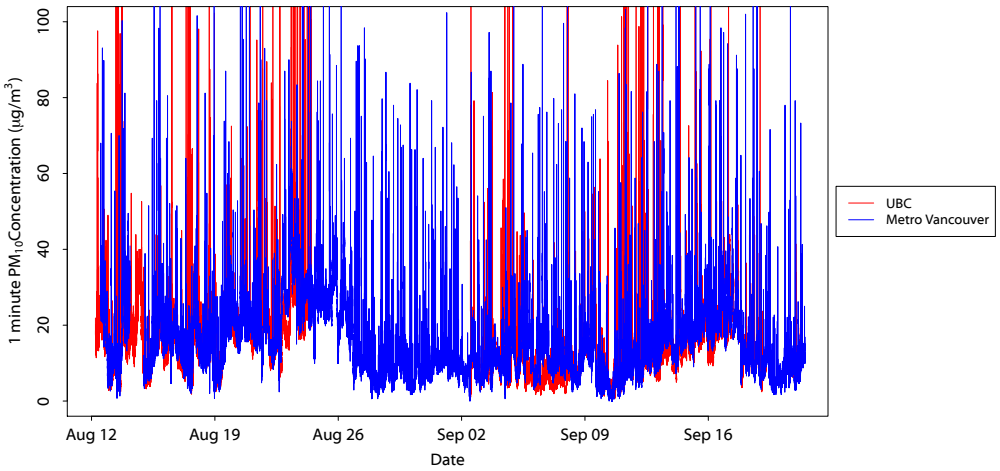

Figure 2.5: Comparison of UBC and MV data, 1 minute averaging time.

Overall, the evidence presented here suggests that the GRIMM data is reliable enough for further analysis, given its satisfactory agreement with a collocated instrument with validated data. Furthermore, using a correction factor of 1 to calculate

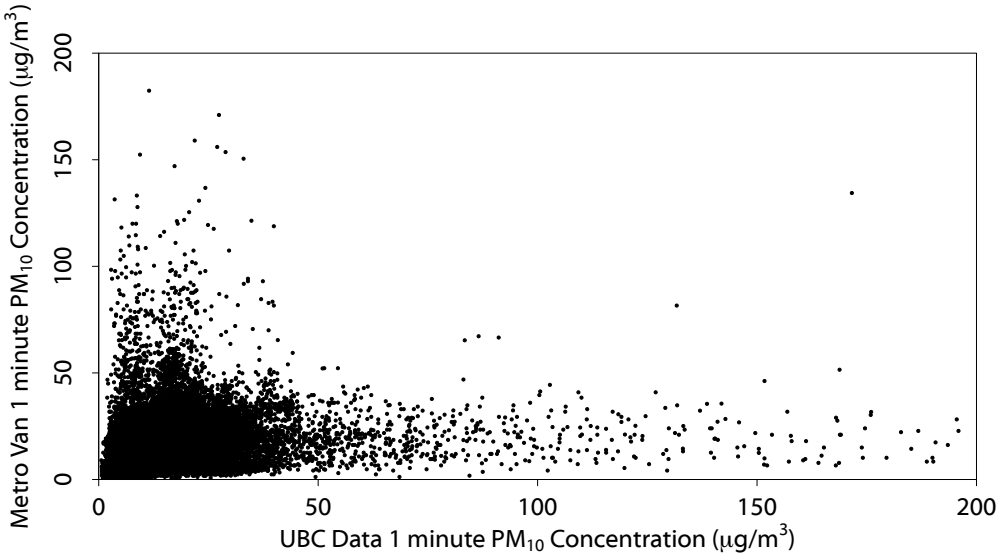

Figure 2.6: Scatterplot of UBC and MV data, 1 minute averaging time.

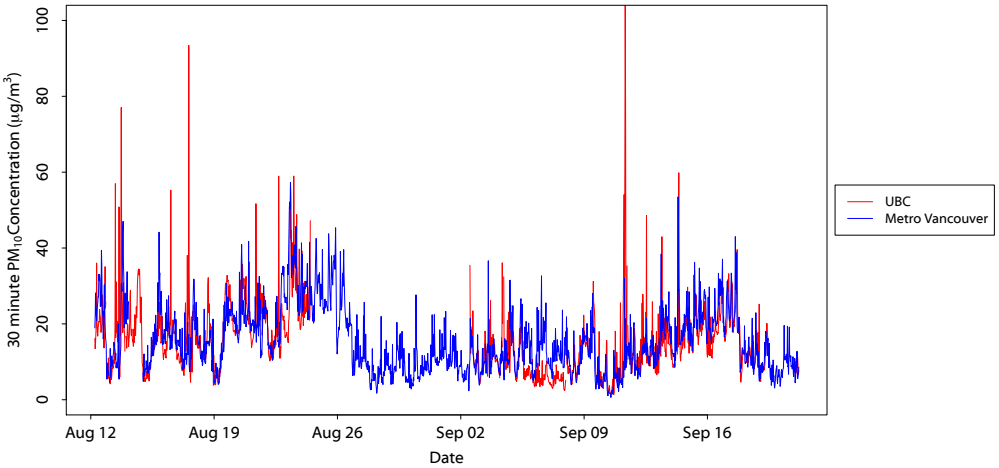

Figure 2.7: Comparison of UBC and MV data, 30 minute averaging time.

mass concentration is a reasonable assumption for the purposes of this study.

2.1.4 Train Passages

In order to determine whether an enhancement of PM concentration is present during a train passage, the time scale must be first determined. Each train passage must be associated with a certain amount of time where PM measurements would

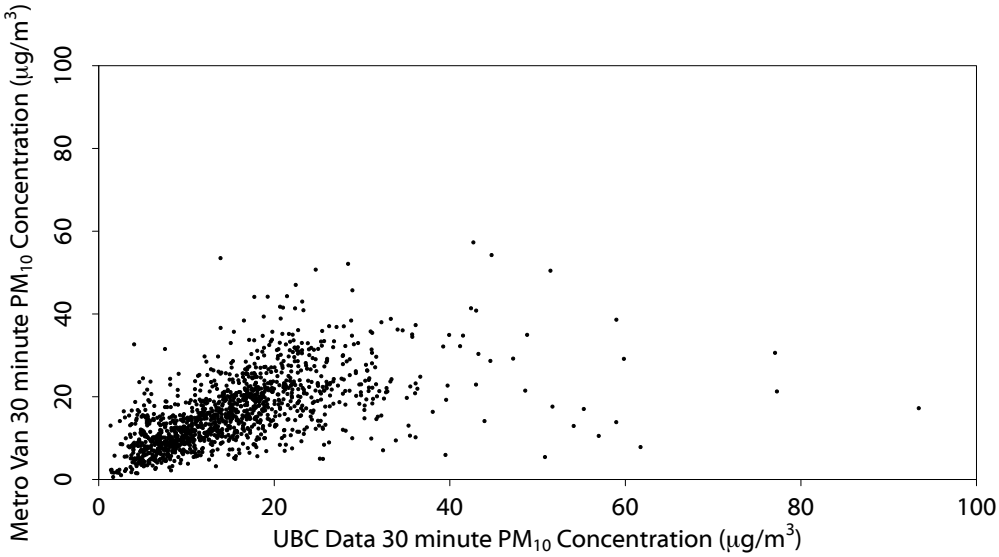

Figure 2.8: Scatterplot of UBC and MV data, 30 minute averaging time.

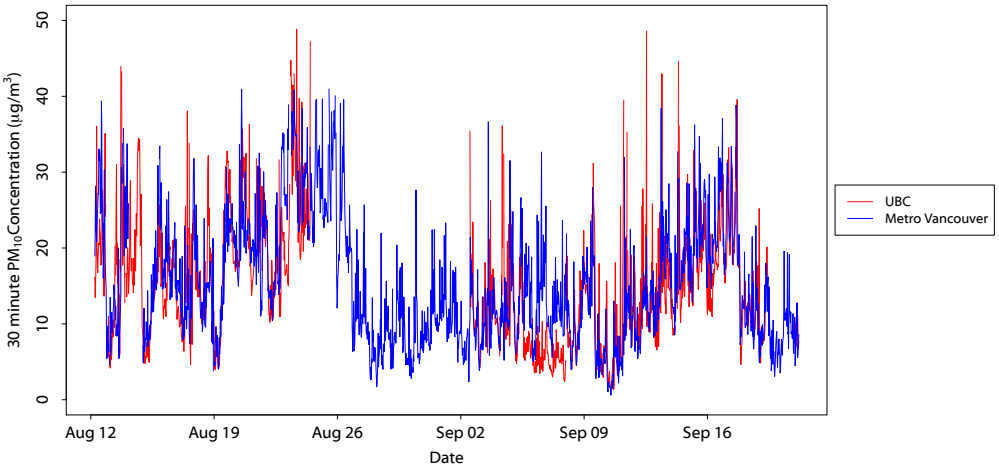

Figure 2.9: Comparison of UBC and MV data, 30 minute averaging time, 99th percentile cutoff.

supposedly be affected by the train passage. This period of time is not static and is dependent on a wide range of factors, including meteorological conditions, instrumentation, train speed, etc. Previous studies ((Jaffe et al., 2014), (Higginbotham et al., 2013)) have detected increases of pollutant concentrations that appear to last on the order of minutes. In these studies, any purported effect by a passing train

Table 2.3: Comparison of GRIMM and E-Sampler Measurements for PM_{10} concentration. 1 minute averaging time.

Instrument	n	Mean	Median	Standard Deviation
GRIMM	42433	15.80 μg/m^3	13.61 μg/m^3	15.61 μg/m^3
E-Sampler	57851	13.93 μg/m^3	11.60 μg/m^3	9.72 μg/m^3

was seen within 10 minutes of the passage of a train.

Due to this, the analysis in this study will use 10 minutes as an approximation for the time period of influence of a passing train. Based on the train audio data collected, as well as visual confirmation, trains at the study site took approximately 4-5 minutes to completely pass. There were some observed instances of just individual locomotives (without any cars attached) passing by the site, but these were not considered as train passages. There was consistency across all trains with regards to speed and time taken to completely pass the site. In order to account for any desynchronization of measurements between the GRIMM and the microphone, it has been assumed that the time period of influence for each individual train passage lasted 14 minutes. This 14 minute period consists of the train passage itself (4 minutes), and two 5-minute buffers before and after the train passage.

The PM concentrations of this 14 minute period of influence can then be compared to control data, representing the background PM concentrations. Since there are numerous confounding factors (meteorology, vehicular traffic, etc.), the control data was defined as a 10 minute period before and after the 14 minute period of influence associated with each train passage. This was done to try and minimize the effects of changing meteorology or vehicular traffic, due to the variable nature of these factors on an hourly scale (Section 3.1). Furthermore, if the control data for a certain train passage happened to coincide with the period of influence of another train passage, the overlapping data was not included in the control data set.

Chapter 3

Influence of Train Passages on PM Concentrations

This chapter aims to identify the effect that passing trains have on observed PM concentrations. This analysis will be conducted by first examining background trends for the purpose of isolating typical patterns in the PM data in order to more accurately discriminate the effect of passing trains. The main statistical analyses used in this chapter are two Analysis of Variance (ANOVA) procedures: one with the data stratified by train type, and the other with the data stratified by train type and wind direction. The results of these analyses are then compared to *in situ* dustfall measurements conducted by the Corporation of Delta. Finally, the PM concentration data recorded by Metro Vancouver at two different distances from the railway is analyzed to isolate any evident spatial trends.

3.1 Background Trends

3.1.1 Diurnal Scale

Outdoor PM concentrations exhibit a typical diurnal pattern as a result of changes in both meteorology and source patterns. In order to examine these diurnal patterns, all of the PM data was aggregated and then isolated by hour of the day. For this diurnal scale analysis, the influence of passing trains is likely obscured by the more persistent trends of vehicular traffic on BC Highway 99 to the south of the park.

The patterns of vehicular traffic on Highway 99 can be analyzed using traffic

data obtained from the BC Ministry of Transportation. Based on these data, it appears that traffic on the highway is in agreement with expectations, with overall volumes reaching a maximum during rush hour periods. However, since observed concentrations are also affected by local meteorological conditions, the observed data may not necessarily mirror the traffic patterns. For example, while vehicular traffic (and therefore, emissions) reach a local maximum during the afternoon rush hour, this corresponds with the time of day with the highest amount of atmospheric mixing, serving to dilute pollutants and reduce observed PM concentrations.

The mean traffic counts and mean PM concentrations sorted by hour of the day are plotted in Figures 3.1 and 3.2, respectively. From these figures, it appears that the distribution of traffic on Highway 99 is bimodal in nature (as expected). The PM concentrations, however, seem to follow a diurnal pattern with relatively high concentrations overnight, steadily decreasing into the afternoon, and then increasing during the evening. This distribution is consistent with the diurnal pattern of dispersion through the atmosphere (McKendry, 2000). It is likely that despite the heavier traffic during the afternoon rush hour, the daytime heating of the surface increases mixing, thereby offsetting the increase in emissions.

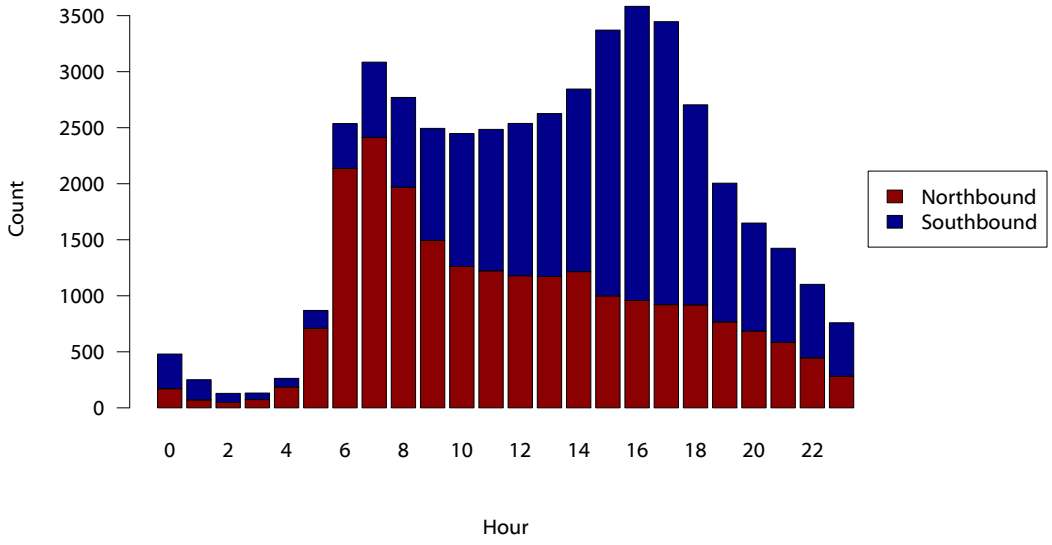

Figure 3.1: Traffic counts on Highway 99 near John Oliver Park for September 2014, sorted by hour.

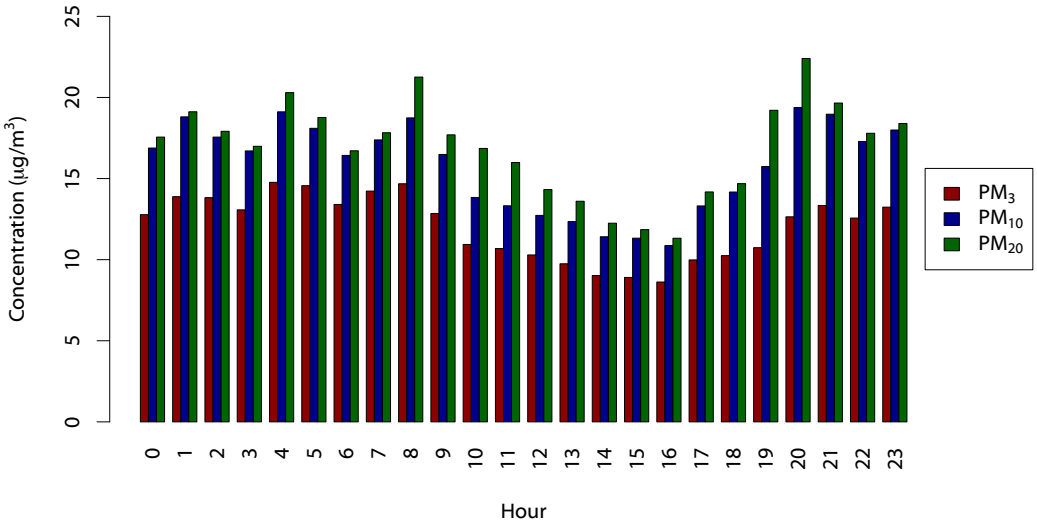

Figure 3.2: Mean PM concentrations recorded at John Oliver Park from 2014-08-14 to 2014-09-21, sorted by hour. Combination of GRIMM and E-Sampler data.

3.1.2 Weekly Scale

If the same traffic and PM concentration data is sorted by day of the week, patterns on a weekly scale can be identified. As expected, traffic counts appear to be slightly lower on weekends compared to weekdays (Figure 3.3). Interestingly, PM concentrations (Figure 3.4) do not exhibit the same pattern. Concentrations appear to be highest on Thursdays, with the lowest concentration days being Monday and Friday. It does not appear that weekends are associated with the lowest mean PM concentrations.

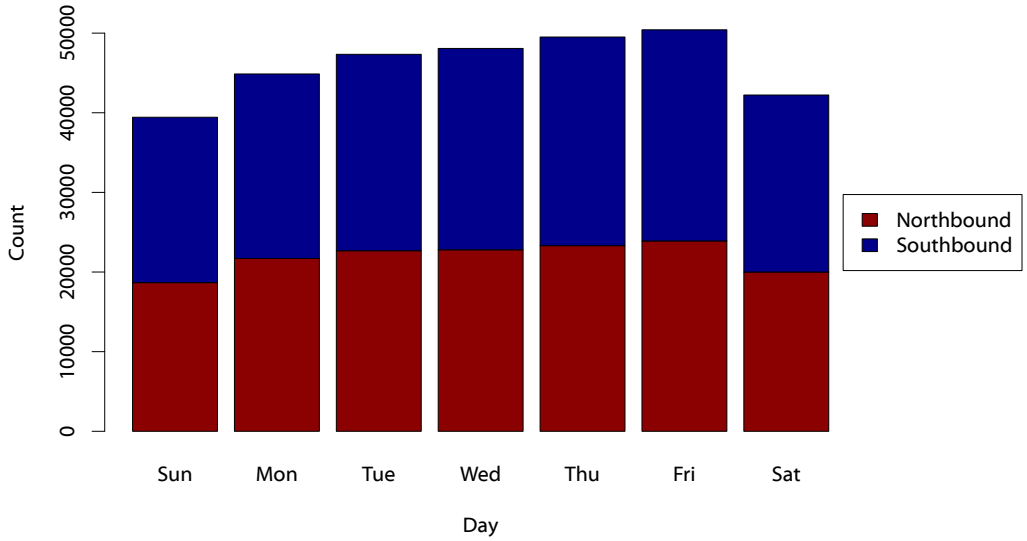

Figure 3.3: Traffic counts on Highway 99 near John Oliver Park for September 2014, sorted by day.

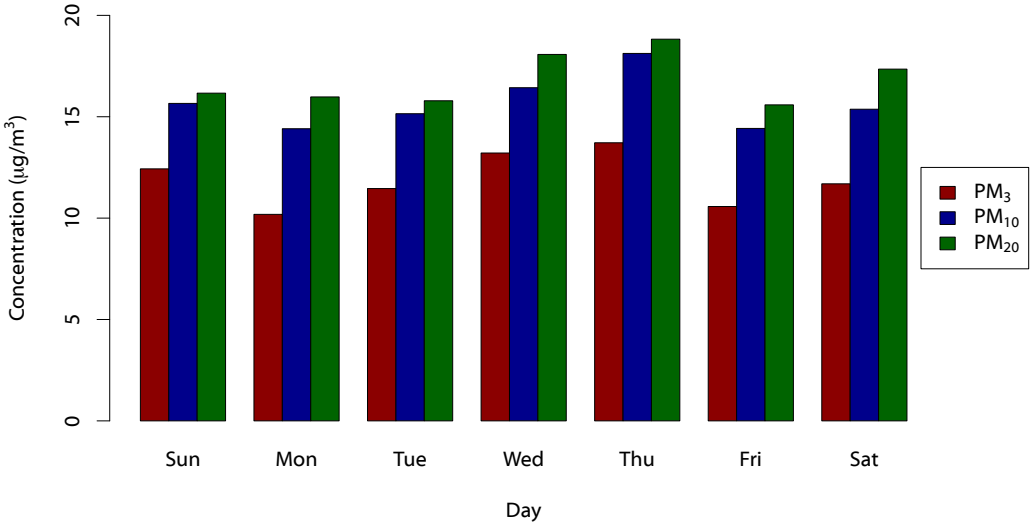

Figure 3.4: Mean PM concentrations recorded at John Oliver Park from 2014-08-14 to 2014-09-21, sorted by day. Combination of GRIMM and E-Sampler data.

3.1.3 Wind Data

John Oliver Park is situated to the north of Boundary Bay, a large body of water that is a major factor controlling the flow regimes of this site. These flow regimes exhibit a strong diurnal cycle, likely driven by a sea breeze-land breeze circulation pattern (Steyn et al., 1997). The daytime wind patterns are dominated by southerly flow coming off of the water, across Highway 99 and the railway, and towards the instruments set up as part of this study (Figure 3.5). Wind speeds are generally light (93.7 % of the time the wind speed is lower than 2 m/s), and higher wind speeds are associated with wind directions from the west. The nighttime regime, in contrast, features a dominantly easterly flow (Figure 3.6), with overall lower wind speeds (98.6 % of wind speeds are lower than 2 m/s). The proportion of data in each wind speed and direction bin is compared between day and night in Table 3.1.

Table 3.1: Comparison of wind data distribution from 2014-08-12 to 2014-09-21 between daytime and nighttime.

Day	**45°**	**90°**	**135°**	**180°**	**225°**	**270°**	**315°**	**360°**
0-1 m/s (%)	1.62	3.52	8.13	24.00	6.57	5.18	2.50	1.32
1-2 m/s (%)	0.35	1.78	1.62	20.22	6.95	6.99	2.66	0.30
2-3 m/s (%)	0.17	0.46	0.07	0.05	0.65	2.68	1.86	0.03
3-4 m/s (%)	0.02	0.02	0.00	0.00	0.05	0.11	0.12	0.00
4-5 m/s (%)	0.00	0.00	0.00	0.00	0.00	0.00	0.00	0.00
Night	**45°**	**90°**	**135°**	**180°**	**225°**	**270°**	**315°**	**360°**
0-1 m/s (%)	7.23	27.79	18.37	10.61	4.66	7.51	6.85	6.35
1-2 m/s (%)	1.05	5.31	0.65	0.84	0.63	0.16	0.08	0.10
2-3 m/s (%)	0.65	0.48	0.00	0.00	0.05	0.01	0.00	0.00
3-4 m/s (%)	0.13	0.07	0.00	0.00	0.00	0.00	0.00	0.00
4-5 m/s (%)	0.00	0.01	0.00	0.00	0.00	0.00	0.00	0.00

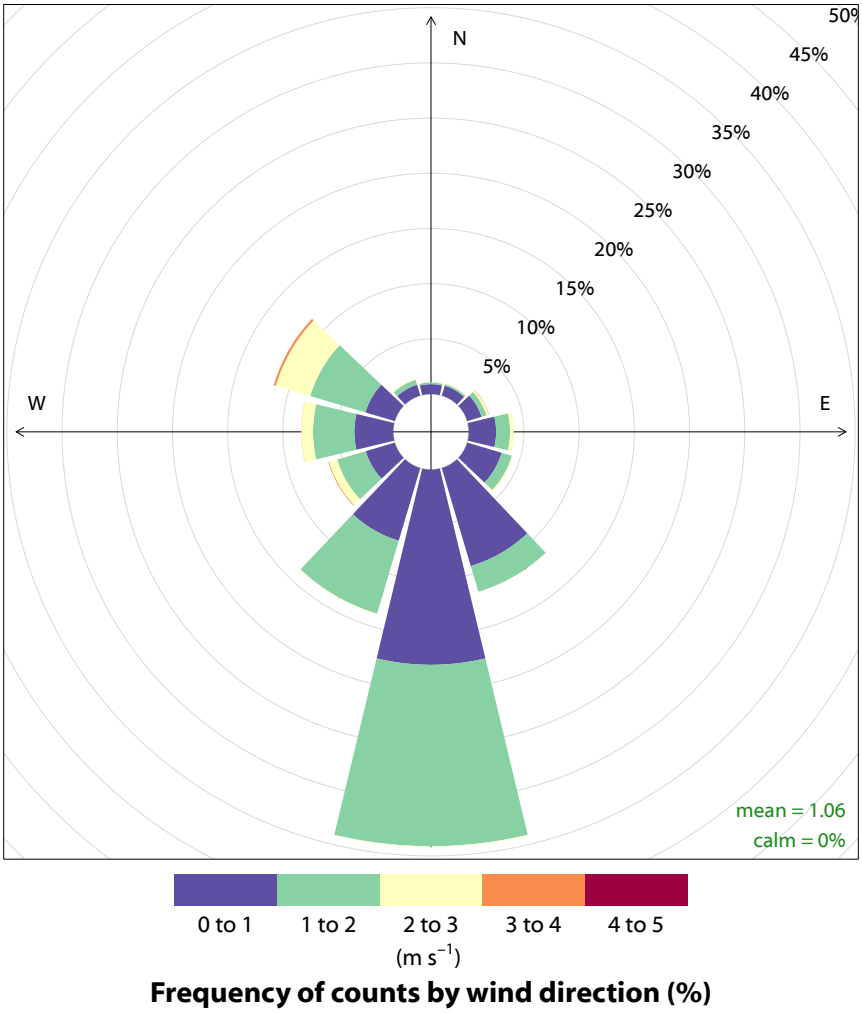

Figure 3.5: Summary of wind data from 2014-08-12 to 2014-09-21 for daytime hours (07:00 - 21:00) at John Oliver Park. Recorded by Metro Vancouver

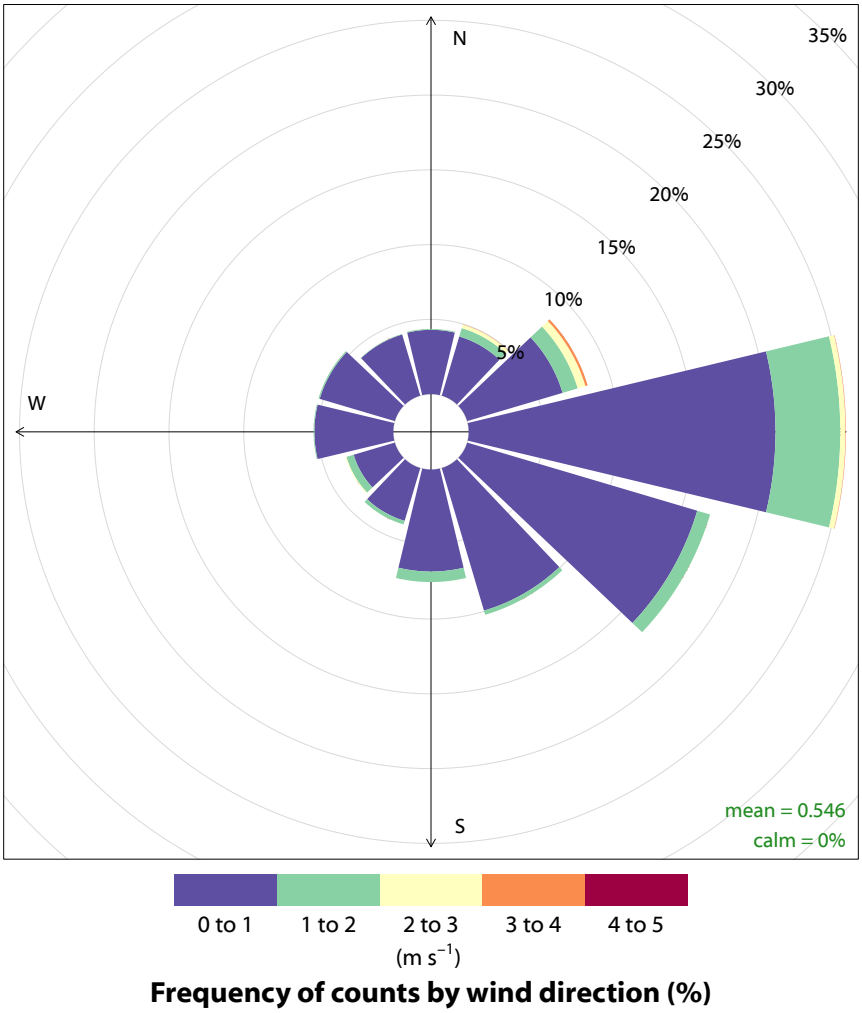

Figure 3.6: Summary of wind data from 2014-08-12 to 2014-09-21 for night-time hours (21:00 - 07:00) at John Oliver Park. Recorded by Metro Vancouver

3.2 Train Traffic

Over the course of the study period, a combination of direct and indirect methods recorded the passage of 408 individual trains by the study site. Of this total, 42 trains were directly visually identified. The remainder of train passages were indirectly recorded using audio data. There does not appear to be any significant trend when the observed trains are sorted by hour (Figure 3.7). It appears that train passages occur at all times during the day. There is potentially a lower amount of traffic during rush hour times in the morning and evening, but more specific data is likely needed to confirm this. When the data is stratified by day of the week, no significant trend is evident (Figure 3.8). The data displayed shows a higher number of trains being recorded on Thursdays, Fridays, and Saturdays, and a much lower train frequency being seen on Mondays. Once again however, train scheduling is dependent on numerous factors that have not been explored here, and more data is likely needed to confirm these trends. Nevertheless, based on these observations, the train traffic at John Oliver Park appears to be somewhat random in nature.

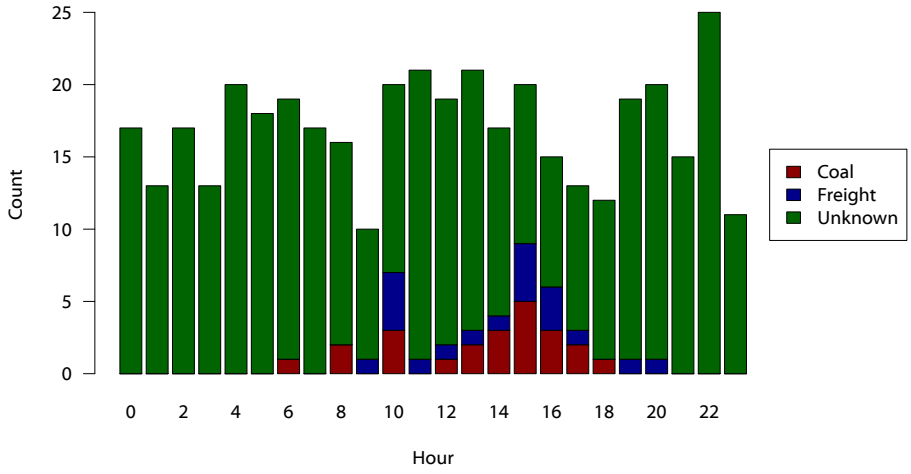

Figure 3.7: Train passages recorded at John Oliver Park from 2014-08-12 to 2014-09-21, sorted by hour. Combination of visual observations and audio recordings.

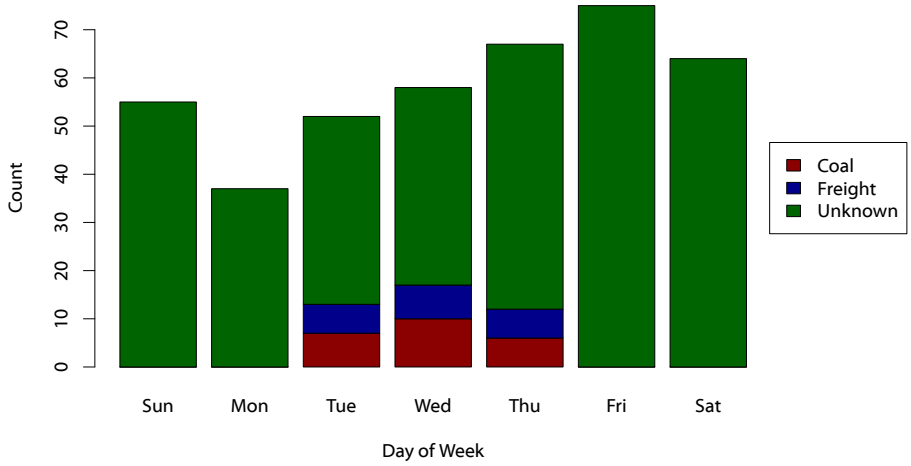

Figure 3.8: Train passages recorded at John Oliver Park from 2014-08-12 to 2014-09-21, sorted by day. Combination of visual observations and audio recordings.

3.3 Particulate Matter Concentration

3.3.1 Effect of Passing Trains (All Types)

Detecting any enhancement of PM concentration during a train passage is simply a matter of combining the PM concentration and train passage data. Using the methodology outlined in section 2.1.4, the PM concentrations associated with passing trains of all types can be broadly compared against the control data. In order to detect differences across particle sizes, this comparison was done for each of PM_3, PM_{10}, and PM_{20}. Figure 3.9 shows a comparison between the distributions in boxplot form, while Table 3.2 lists basic statistics for each group.

Table 3.2: Basic statistics of PM concentration during train passages versus control data, from 2014-08-12 to 2014-09-21. Combination of GRIMM and E-Sampler data.

Group	**n**	**Mean** (μg/m^3)	**Median** (μg/m^3)	**Std. Dev.** (μg/m^3)
PM_3 Passage	4048	10.38	8.53	8.35
PM_3 Control	4095	10.17	8.48	9.01
PM_{10} Passage	5217	13.16	9.66	16.00
PM_{10} Control	5322	12.68	9.56	16.32
PM_{20} Passage	4048	15.53	11.73	20.88
PM_{20} Control	4095	15.30	11.68	28.12

On first glance, the two distributions appear quite similar across all size ranges. If the means for each distribution are compared using a t-test (with Welch correction for unequal variances), the means for all size ranges are found to be not significantly different from one another at $\alpha = 0.01$ (Table 3.3). A significance level of 0.01 was chosen to use in this analysis to reduce the chance of a Type I error, given the numerous confounding factors that could affect the measurements. Note that for the purposes of these tests, the data was base 10 log transformed to create a distribution closer to normality.

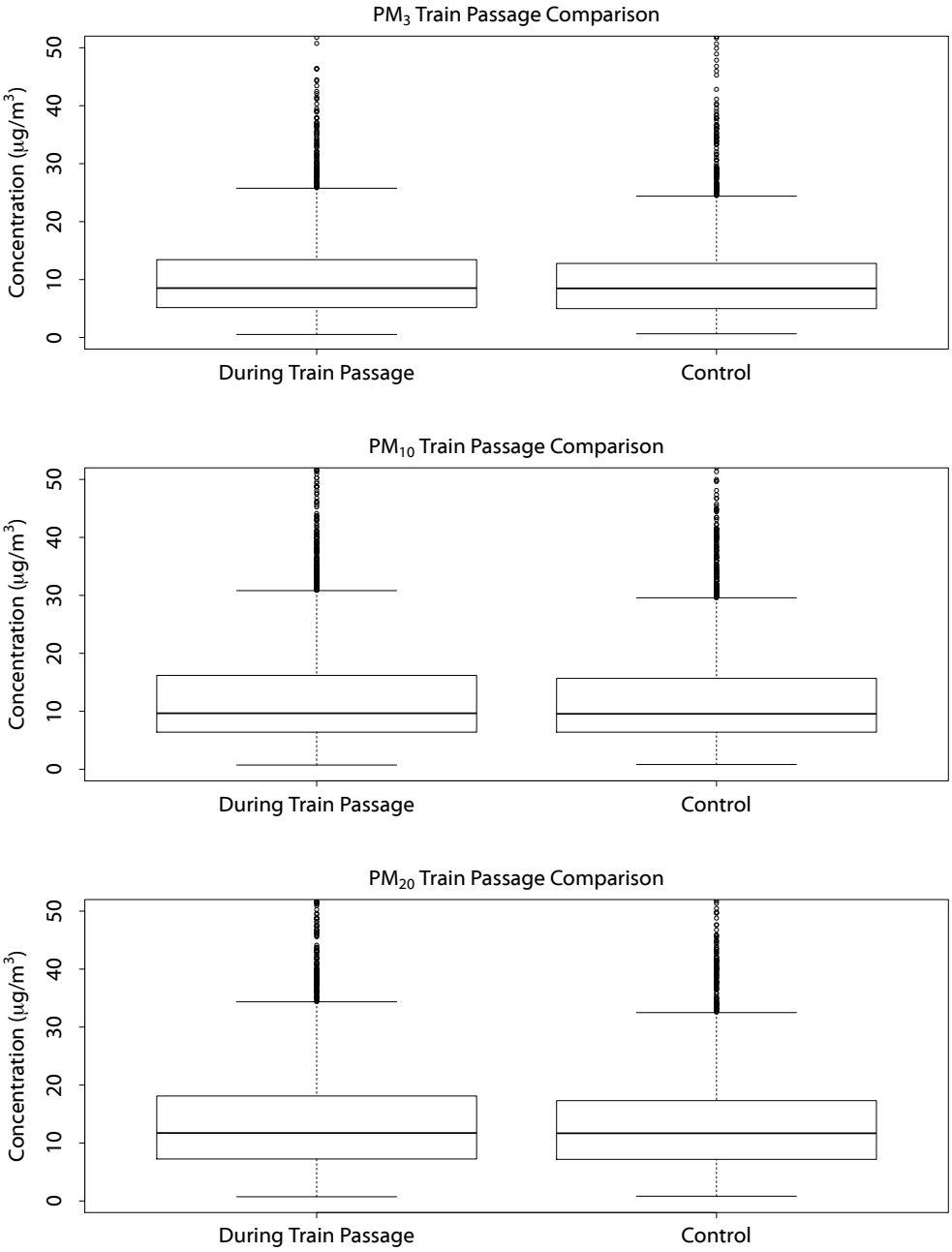

Figure 3.9: Comparison of PM concentration during train passages versus control, from 2014-08-12 to 2014-09-21. Combination of GRIMM and E-Sampler data.

Table 3.3: Welch t-test of differences of means with log transformed data ($_p$ = passage, $_c$ = control). $\alpha = 0.01$,

Comparison	Hypothesis Test	Test Statistic	p-value
PM_3	$\mu_p \neq \mu_c$	1.469	0.142
PM_{10}	$\mu_p \neq \mu_c$	1.007	0.314
PM_{20}	$\mu_p \neq \mu_c$	1.339	0.181

3.3.2 Effect of Passing Trains with Wind Direction

As the wind direction strongly influences observed PM concentrations, we can further analyze the data by taking wind direction into account. The approach used here broadly categorizes wind direction into one of two groups: directions when the instruments are downwind of the railway, and directions when the instruments are upwind of the railway. The specific criteria used here were defined by using the axis of the railway. The railway runs approximately 74° - 254°. Thus, any headings between 74° to 254° represent the wind blowing from the south, across the railway, and towards the instruments set up at the park. Any headings outside of that range would represent the wind blowing from the north, making the instruments upwind of the railway, and therefore unlikely to be influenced by the highway or railway. The convention used in this report will be from the frame of reference of the instruments being either **upwind** or **downwind** with respect to the highway/railway.

Figure 3.10 shows, once again, minimal differences between passage and control groups. However, the effect of wind direction on observed concentrations is quite apparent, with downwind conditions resulting in higher mean concentrations than upwind conditions. Moreover, it appears that the enhancement of mean PM concentration due to downwind conditions gets weaker with larger size ranges. For the control data, downwind conditions result in a mean enhancement of 2.35, 1.57, and 1.70 $\mu g/m^3$ for PM_3, PM_{10}, and PM_{20}, respectively. Another trend that appears in the data is the difference in variability across both size ranges and wind directions. The standard deviation appears to increase with both increasing particle size and downwind conditions (Table 3.4). A larger amount of variability in the data would seem to suggest stronger periodic spikes in concentration. The fact that this is associated with downwind conditions makes sense, since PM blowing from the highway and railway may cause more variability in the recorded data. In contrast, as there

are few strong PM sources at John Oliver Park north of the instrument site, upwind conditions should produce less variability in the data.

Table 3.4: Basic statistics of PM concentration during train passages versus control data, segmented by wind direction, from 2014-08-12 to 2014-09-21. Combination of GRIMM and E-Sampler data.

Group	**n**	**Mean** (g/m^3)	**Median** (g/m^3)	**Std. Dev.** (g/m^3)
PM_3 Passage (Downwind)	2731	10.94	9.33	8.32
PM_3 Control (Downwind)	3523	10.91	9.34	9.78
PM_3 Passage (Upwind)	1317	9.21	6.55	8.30
PM_3 Control (Upwind)	1691	8.56	6.66	6.82
PM_{10} Passage (Downwind)	3632	13.41	10.14	16.06
PM_{10} Control (Downwind)	4751	13.14	10.32	18.28
PM_{10} Passage (Upwind)	1585	12.59	8.52	15.87
PM_{10} Control (Upwind)	2043	11.57	8.45	10.02
PM_{20} Passage (Downwind)	2731	15.86	12.23	21.83
PM_{20} Control (Downwind)	3523	15.83	12.09	31.38
PM_{20} Passage (Upwind)	1317	14.86	10.20	18.75
PM_{20} Control (Upwind)	1691	14.13	10.28	19.25

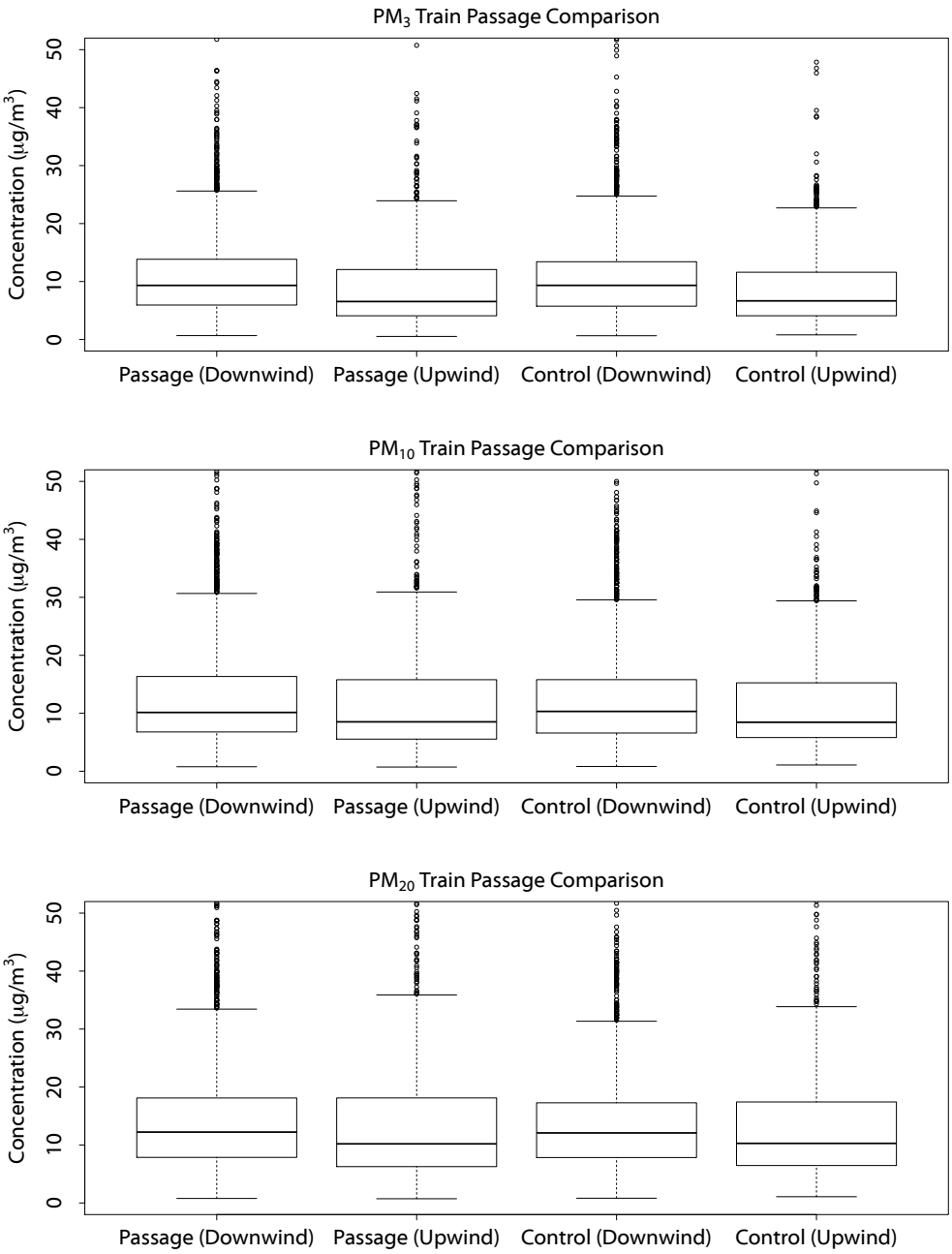

Figure 3.10: Comparison of PM concentration during train passage versus control, stratified by wind direction, from 2014-08-12 to 2014-09-21. Combination of GRIMM and E-Sampler data.

3.3.3 Effect of Passing Coal Trains

Isolating the effect of passing coal trains required comparing PM data to the times of confirmed coal train passages. At certain times, the GRIMM data was found to be unreliable (Section 2.1.3), and given the relatively small number of confirmed coal train passages, the data collected by Metro Vancouver was combined with the GRIMM data for this analysis. While the Metro Vancouver data was recorded at the same location at John Oliver Park (50 m north of the study railway), the E-Sampler instrument used only recorded PM_{10} concentrations. Thus, the PM_{10} data includes all 16 visually confirmed coal train passages (out of 42 visually confirmed passages, and 408 total passages), while the PM_3 and PM_{20} data only includes seven visually confirmed coal train passages (out of 27 visually confirmed passages, and 307 total passages).

Each data set was stratified into three groups: coal train passages, all train passages, and control. The method used to identify membership to these groups is the same as described in Section 2.1.4. It is also important to note that the groups for coal train passages and all train passages are not mutually exclusive; coal train passages are included in the "all trains" group. However, both of these groups are mutually exclusive with the control group. Figures 3.11-3.13 show the distributions of these groups, while Table 3.5 summarizes the basic statistics for each distribution.

As mentioned in Section 3.3.1, the PM data being used here is not normally distributed. As such, a base 10 log transformation was applied to the data to more closely approximate a normal distribution. Before performing an ANOVA to compare the three groups of data, diagnostic tests were used to ensure that ANOVA was appropriate for this data. The diagnostic tests for each of PM_3, PM_{10}, and PM_{20} are shown in Figures 3.14-3.16, respectively.

The normal Q-Q plots show that the data is somewhat normally distributed. However, the assumption of normality can be met by assuming that the central limit theorem holds, given the large sample sizes being used. However, the assumption of homoscedasticity of residuals is more problematic. The residuals vs. fitted plots in Figures 3.14-3.16 show unequal variance across the fitted values. Moreover, using Levene's Test for homogeneity of variance yields a significant p-value at $\alpha = 0.01$ for all PM ranges. This results in rejecting the null hypothesis, suggesting that the data is heteroscedastic. Nevertheless, the one-way ANOVA procedure can still be performed while including a Welch correction for the heteroscedasticity. All size ranges yield a significant p-value at $\alpha = 0.01$, suggesting that the groups (coal trains,

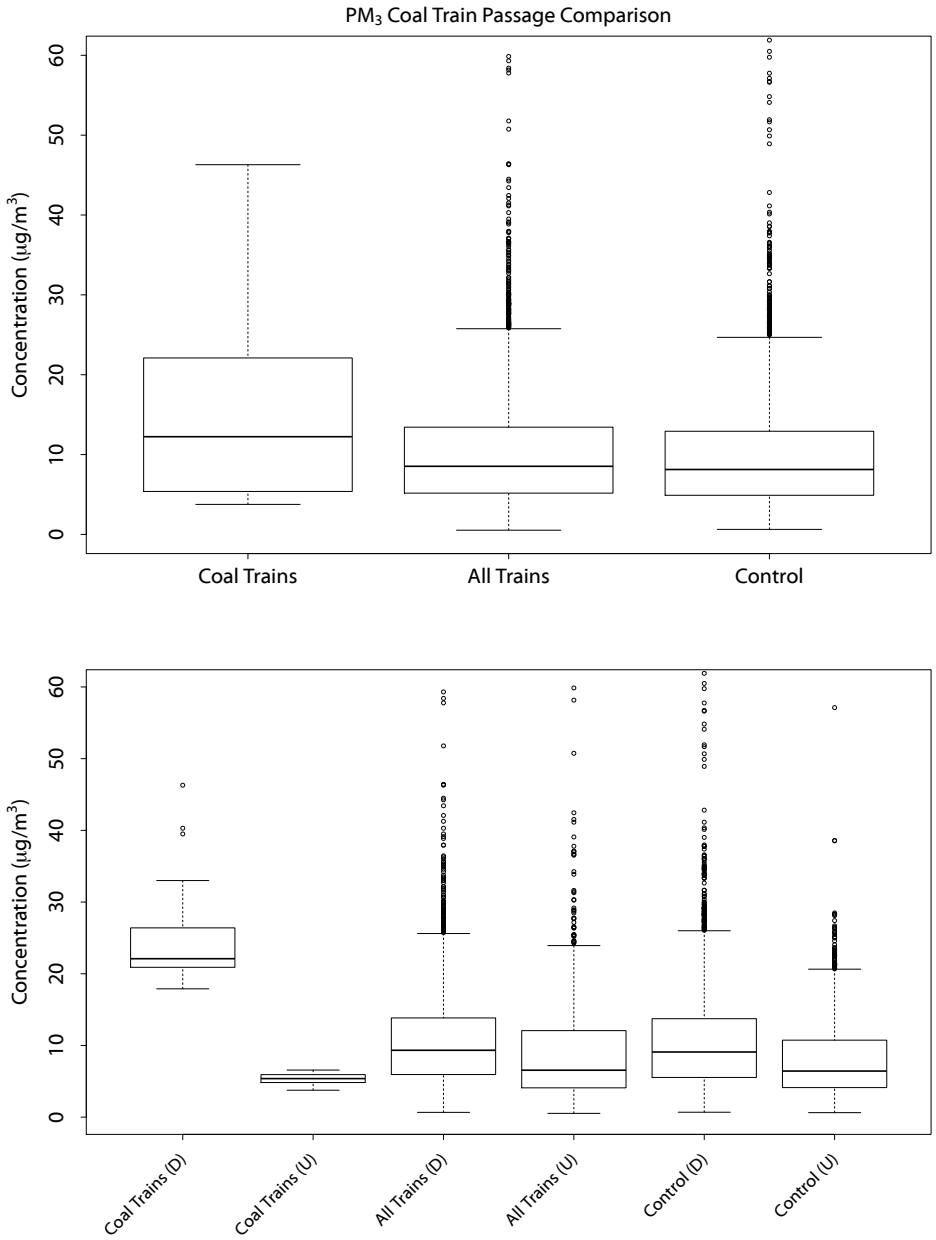

Figure 3.11: Boxplots of each PM_3 group used in ANOVA testing. (D) denotes downwind conditions, while (U) denotes upwind conditions. Combination of data from GRIMM OPC and E-Sampler.

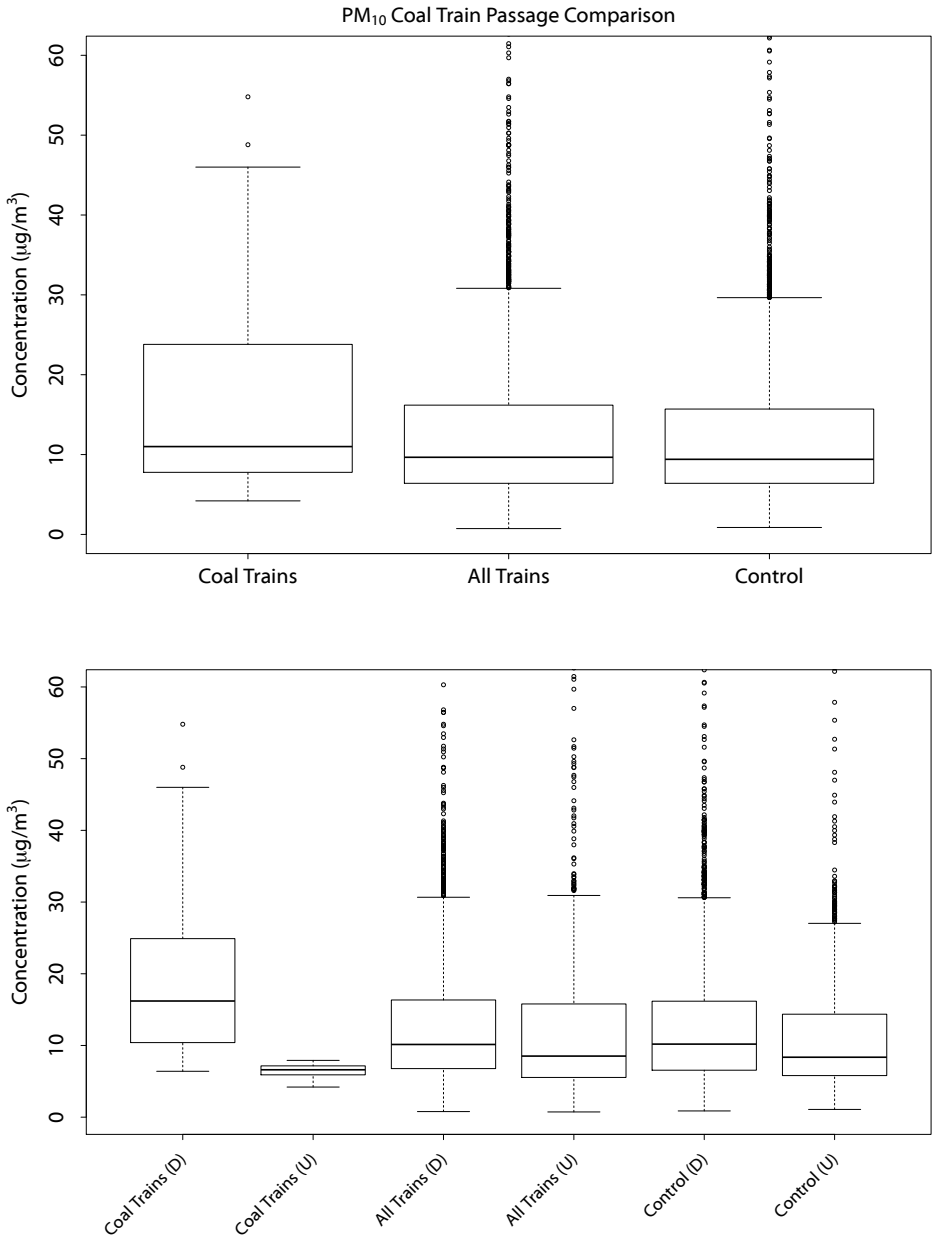

Figure 3.12: Boxplots of each PM_{10} group used in ANOVA testing. (D) denotes downwind conditions, while (U) denotes upwind conditions. Combination of data from GRIMM OPC and E-Sampler.

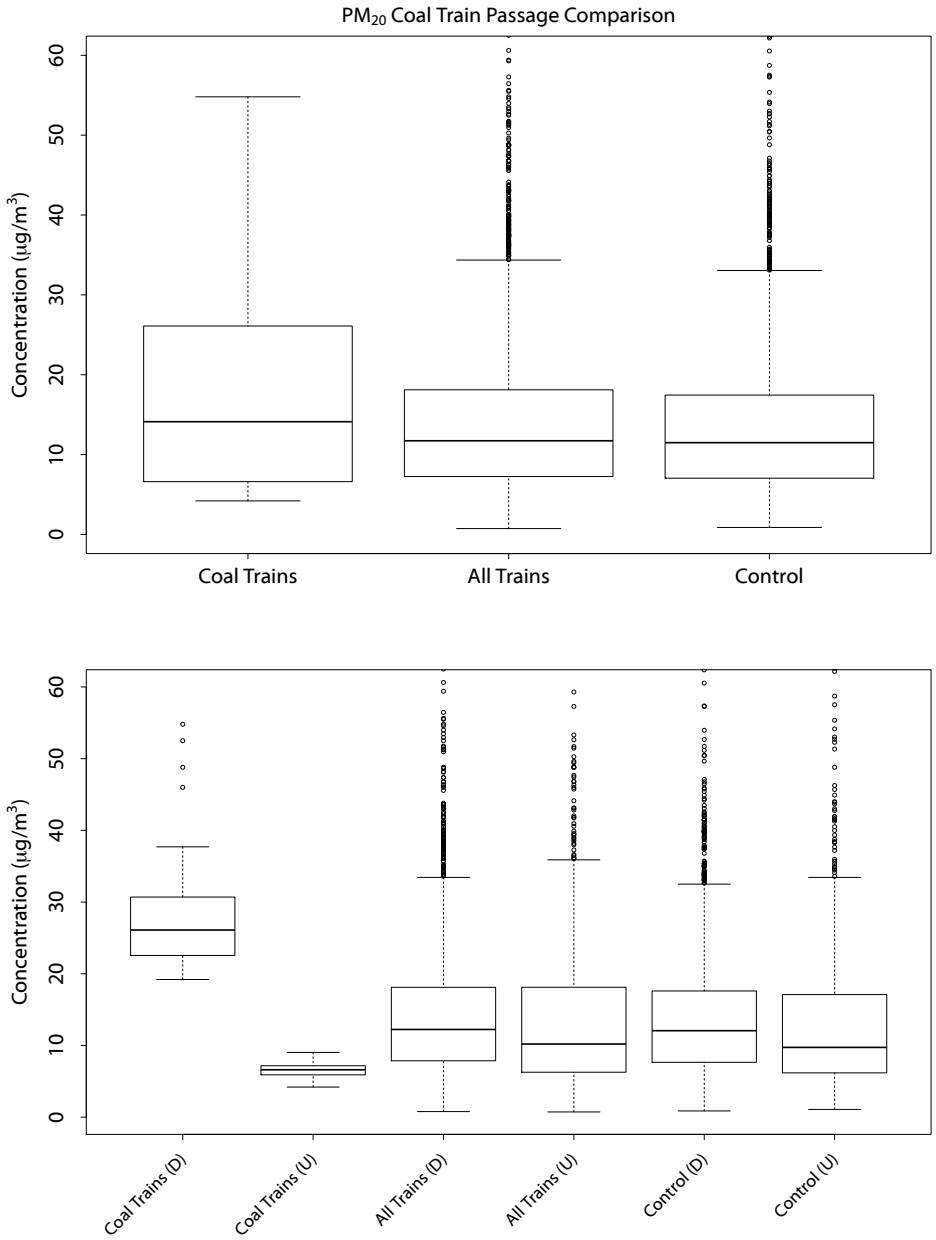

Figure 3.13: Boxplots of each PM_{20} group used in ANOVA testing. (D) denotes downwind conditions, while (U) denotes upwind conditions. Combination of data from GRIMM OPC and E-Sampler.

Table 3.5: Basic statistics of PM concentrations for stratified data, from 2014-08-12 to 2014-09-21. Combination of GRIMM and E-Sampler data.

Group	**n**	**Mean** (g/m^3)	**Median** (g/m^3)	**Std. Dev.** (g/m^3)
PM_3 Coal Trains	78	15.09	12.24	10.75
PM_3 All Trains	4048	10.38	8.53	8.35
PM_3 Control	5214	9.81	8.13	8.09
PM_{10} Coal Trains	200	16.44	11.00	10.26
PM_{10} All Trains	5217	13.16	9.66	16.00
PM_{10} Control	6794	12.33	9.41	14.87
PM_{20} Coal Trains	78	17.53	14.12	12.68
PM_{20} All Trains	4048	15.53	11.73	20.88
PM_{20} Control	5214	14.98	11.49	38.38

all trains, and control) do not belong to the same population (Table 3.6-3.7).

Post-hoc tests (Tables 3.6-3.7) can be used to detect the pairs of groups that are causing the overall significant result for the three size ranges. Due to the unequal variances and sample sizes, the Games-Howell procedure was used for pairwise comparisons. Since there are three pairs of groups, the p-values from these tests are compared against an $\alpha^{'}$ value of 0.0033 ($\alpha/3$). The results of the post-hoc tests differ between the size ranges. For PM_3, all pairs of groups were found to be significantly different from one another. For PM_{10}, the coal train group was found to be significantly different from both the all trains group and the control group, but no significant difference was found between the all trains group and the control group. The PM_{20} post-hoc tests produced interesting results. Despite the overall significant result for the ANOVA test, the post-hoc tests did not find any significant pairwise differences. This suggests that any overall differences between groups may be fairly weak.

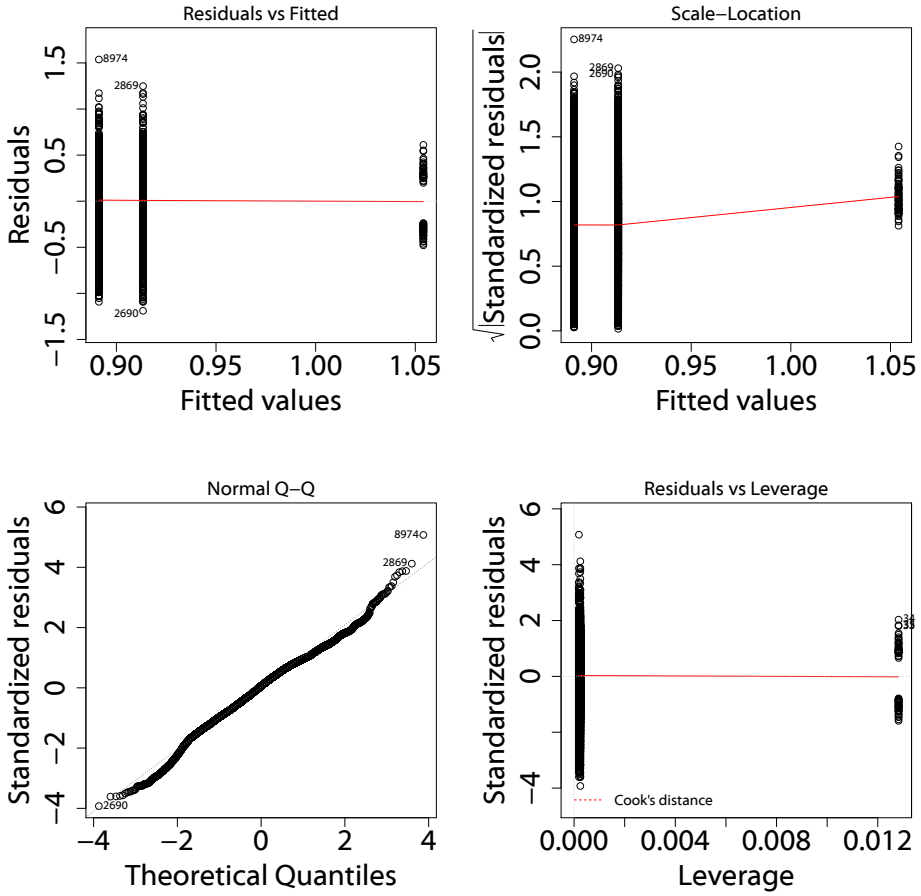

Figure 3.14: ANOVA diagnostic tests for PM_3 data.

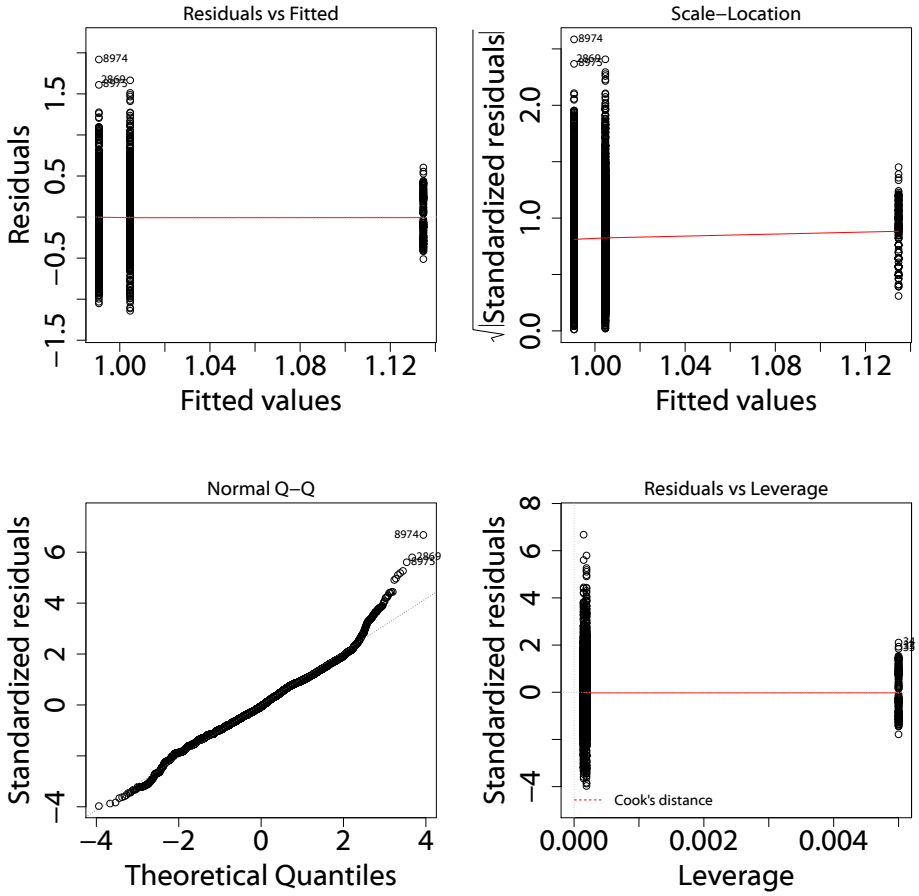

Figure 3.15: ANOVA diagnostic tests for PM_{10} data.

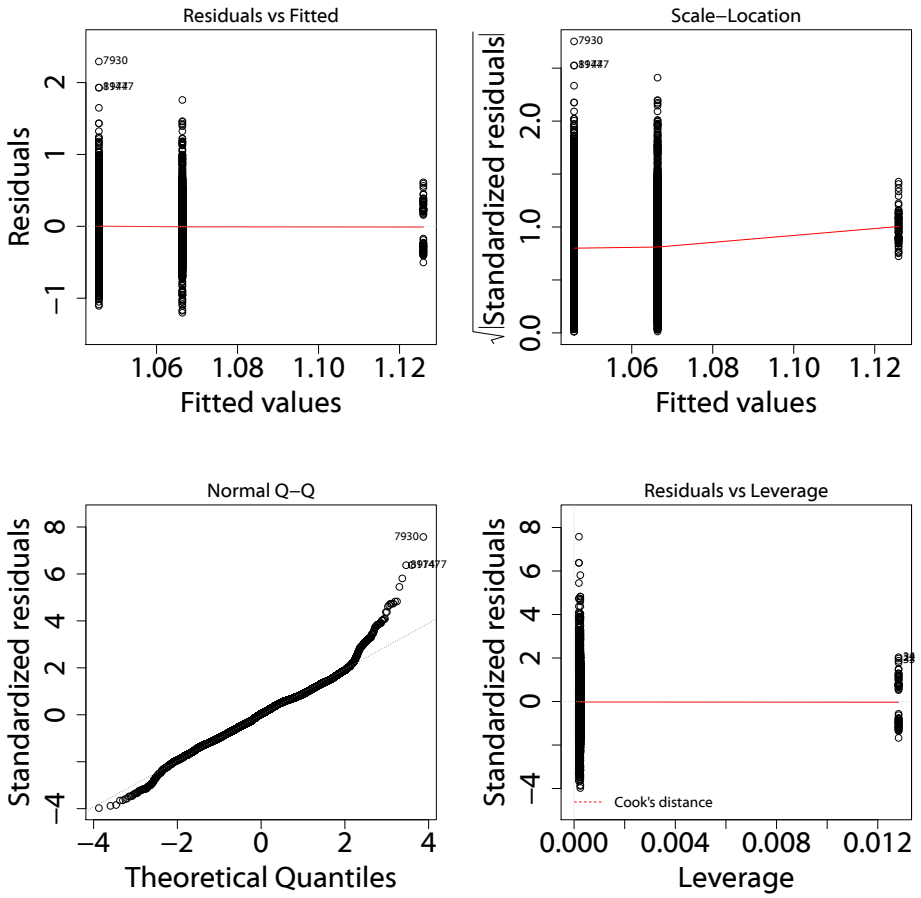

Figure 3.16: ANOVA diagnostic tests for PM_{20} data.

Table 3.6: Summary of parametric hypothesis testing for log-transformed PM_3 data. $\alpha = 0.01$, $\alpha^{'} = 0.01/3 = 0.00333$

Test	**Hypotheses**	**p-value**	**Reject H_0?**
Shapiro-Wilk	H_0: The data is normal H_1: The data is not normal	< 0.0001	Yes
Levene's Test	H_0: Variances equal across groups H_1: Variances not equal across groups	< 0.0001	Yes
One-Way ANOVA	H_0: $\mu_{coal} = \mu_{all} = \mu_{control}$ H_1: $\mu_{coal} \neq \mu_{all} \neq \mu_{control}$	0.0022	Yes
Games-Howell Post-Hoc	H_0: $\mu_{coal} = \mu_{all}$ H_1: $\mu_{coal} \neq \mu_{all}$	0.002	Yes
	H_0: $\mu_{coal} = \mu_{control}$ H_1: $\mu_{coal} \neq \mu_{control}$	0.0002	Yes
	H_0: $\mu_{all} = \mu_{control}$ H_1: $\mu_{all} \neq \mu_{control}$	0.001	Yes

Table 3.7: Summary of parametric hypothesis testing for log-transformed PM_{10} data. $\alpha = 0.01$, $\alpha^{'} = 0.01/3 = 0.00333$

Test	**Hypotheses**	**p-value**	**Reject H_0?**
Shapiro-Wilk	H_0: The data is normal H_1: The data is not normal	< 0.0001	Yes
Levene's Test	H_0: Variances equal across groups H_1: Variances not equal across groups	< 0.0001	Yes
One-Way ANOVA	H_0: $\mu_{coal} = \mu_{all} = \mu_{control}$ H_1: $\mu_{coal} \neq \mu_{all} \neq \mu_{control}$	< 0.0001	Yes
Games-Howell Post-Hoc	H_0: $\mu_{coal} = \mu_{all}$ H_1: $\mu_{coal} \neq \mu_{all}$	< 0.0001	Yes
	H_0: $\mu_{coal} = \mu_{control}$ H_1: $\mu_{coal} \neq \mu_{control}$	< 0.0001	Yes
	H_0: $\mu_{all} = \mu_{control}$ H_1: $\mu_{all} \neq \mu_{control}$	0.0248	No

Table 3.8: Summary of parametric hypothesis testing for log-transformed PM_{20} data. $\alpha = 0.01$, $\alpha^{'} = 0.01/3 = 0.00333$

Test	**Hypotheses**	**p-value**	**Reject H_0?**
Shapiro-Wilk	H_0: The data is normal H_1: The data is not normal	< 0.0001	Yes
Levene's Test	H_0: Variances equal across groups H_1: Variances not equal across groups	< 0.0001	Yes
One-Way ANOVA	H_0: $\mu_{coal} = \mu_{all} = \mu_{control}$ H_1: $\mu_{coal} \neq \mu_{all} \neq \mu_{control}$	0.001	Yes
Games-Howell Post-Hoc	H_0: $\mu_{coal} = \mu_{all}$ H_1: $\mu_{coal} \neq \mu_{all}$	0.26	No
	H_0: $\mu_{coal} = \mu_{control}$ H_1: $\mu_{coal} \neq \mu_{control}$	0.087	No
	H_0: $\mu_{all} = \mu_{control}$ H_1: $\mu_{all} \neq \mu_{control}$	0.0034	No

3.3.4 Effect of Passing Coal Trains with Wind Direction

Using the same methodology as in 3.3.2, the data can be further stratified by wind direction (the instruments being downwind or upwind of the railway). Given the relative lack of data for PM_3 and PM_{20} that coincides with coal train passages, this analysis will only be performed on the PM_{10} data. The distributions of these six groups are shown in Figure 3.12. From the boxplots, it appears that the downwind coal train group is associated with higher PM_{10} concentrations than the other groups. Moreover, the effect of wind direction is also visible here, with downwind conditions resulting in higher concentrations than upwind conditions. Interestingly, the group with the smallest median value is the upwind coal train group. However, this could be explained by a lack of data (only 4 train passages satisfy this criterion). The basic statistics of each group is summarized in Table 3.9.

Similar to Section 3.3.3, the diagnostic plots in Figure 3.17 show that the data exhibits both non-normality and heteroscedasticity to a certain degree. The Shapiro-Wilk test suggests that the data is significantly different from normally distributed, while Levene's Test suggests that the data is not homoscedastic. Therefore, the One-Way ANOVA with a Welch correction was used to test for differences between each group, assuming that normality holds due to the central limit theorem. The significant result in the ANOVA analysis leads to post-hoc testing using the Games-Howell procedure. The results of the post-hoc testing are summarized in Table 3.11 (a significance level of $\alpha^{'} = 0.01/15 = 0.00067$ has been assumed).

The results of the post-hoc test show that the only pairs of groups that do not have significantly different means are: Coal (Upwind) and Control (Upwind); All Trains (Downwind) and Control (Downwind); and All Trains (Upwind) and Control (Upwind). The overall trend in significance in Table 3.11 suggest that both wind direction and coal train passages are causing the overall significant result. This is in agreement with the previous analyses conducted in this chapter.

Table 3.9: Basic statistics of PM_{10} concentration data, stratified by wind, from 2014-08-12 to 2014-09-21. Combination of GRIMM and E-Sampler data.

Group	**n**	**Mean** (g/m^3)	**Median** (g/m^3)	**Std. Dev.** (g/m^3)
Coal Trains (Downwind)	161	18.85	16.20	10.05
Coal Trains (Upwind)	39	6.52	6.61	0.88
All Trains (Downwind)	3632	13.41	10.14	16.06
All Trains (Upwind)	1585	12.59	8.52	15.87
Control (Downwind)	4751	12.85	10.19	16.55
Control (Upwind)	2043	11.12	8.36	9.80

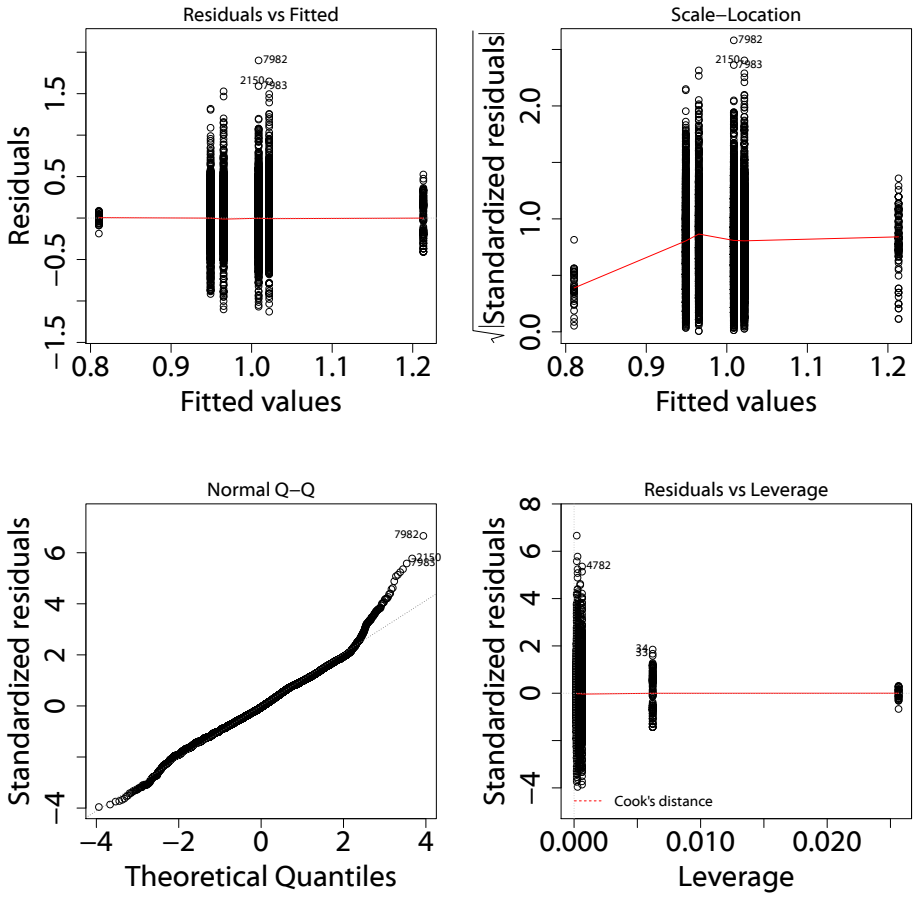

Figure 3.17: Diagnostic tests for ANOVA testing, stratified by wind.

Table 3.10: Summary of parametric hypothesis testing for PM_{10} data, stratified by wind. $\alpha = 0.01$

Test	Hypotheses	p-value	Result
Shapiro-Wilk	H_0: The data is normal H_1: The data is not normal	< 0.0001	Reject H_0
Levene's Test	H_0: Variances equal across groups H_1: Variances not equal across groups	< 0.0001	Reject H_0
One-Way ANOVA	H_0: All groups have equal means H_1: At least one group's mean is not equal	< 0.0001	Reject H_0

Table 3.11: Summary of Games-Howell post-hoc analysis for PM_{10} data, stratified by wind. Subscripts: D = Downwind, U = Upwind. $\alpha^{'} = 0.01/15 = 0.00067$

H_0	H_1	p-value	Reject H_0?
$\mu_{coalD} = \mu_{coalU}$	$\mu_{coalD} \neq \mu_{coalU}$	< 0.0001	Yes
$\mu_{coalD} = \mu_{allD}$	$\mu_{coalD} \neq \mu_{allD}$	< 0.0001	Yes
$\mu_{coalD} = \mu_{allU}$	$\mu_{coalD} \neq \mu_{allU}$	< 0.0001	Yes
$\mu_{coalD} = \mu_{controlD}$	$\mu_{coalD} \neq \mu_{controlD}$	< 0.0001	Yes
$\mu_{coalD} = \mu_{controlU}$	$\mu_{coalD} \neq \mu_{controlU}$	< 0.0001	Yes
$\mu_{coalU} = \mu_{allD}$	$\mu_{coalU} \neq \mu_{allD}$	< 0.0001	Yes
$\mu_{coalU} = \mu_{allU}$	$\mu_{coalU} \neq \mu_{allU}$	< 0.0001	Yes
$\mu_{coalU} = \mu_{controlD}$	$\mu_{coalU} \neq \mu_{controlD}$	< 0.0001	Yes
$\mu_{coalU} = \mu_{controlU}$	$\mu_{coalU} \neq \mu_{controlU}$	< 0.0001	No
$\mu_{allD} = \mu_{allU}$	$\mu_{allD} \neq \mu_{allU}$	< 0.0001	Yes
$\mu_{allD} = \mu_{controlD}$	$\mu_{allD} \neq \mu_{controlD}$	0.273	No
$\mu_{allD} = \mu_{controlU}$	$\mu_{allD} \neq \mu_{controlU}$	< 0.0001	Yes
$\mu_{allU} = \mu_{controlD}$	$\mu_{allU} \neq \mu_{controlD}$	< 0.0001	Yes
$\mu_{allU} = \mu_{controlU}$	$\mu_{allU} \neq \mu_{controlU}$	0.609	No
$\mu_{controlD} = \mu_{controlU}$	$\mu_{controlD} \neq \mu_{controlU}$	< 0.0001	Yes

3.4 Dustfall Measurements

The final part of the results from this study includes passive sampling undertaken by the Corporation of Delta. The sampling campaign took place over the course of one year, with analysis being done every three months. Each analysis was on a sample collected over the course of one month (April 2014, July 2014, October 2014, and January 2015). The aim of this project was to determine the proportion of the sample that was coal dust. The following section will focus on the July 2014 analysis, given the similar timeframe to the other data collected at John Oliver Park. A summary of the results from July 2014 is provided in Table 3.12.

The results for April and July 2014 clearly show the presence of coal dust at the John Oliver Park site. Moreover, out of five locations examined by this study, the only two locations with large proportions ($> 10\%$) of coal particles present were directly adjacent to the railway. This clearly suggests a relationship between the railway in question and the generation of coal dust. The current BC Air Quality guidelines for dustfall in a non-residential area is 2.9 mg/dm^2/day. Based on the analysis for July 2014, the John Oliver Park site exceeded this guideline by 1.81 mg/dm^2/day. Due to the high proportion of coal particles in the sample, it appears that the exceedance of the guideline is due to the coal dust found at the site. Interestingly, it appears that the amount of dustfall drastically decreases into the autumn and winter months. Given the dependency of measured PM on meteorological conditions, it is possible that this change is due to a change in day-to-day local meteorology. Indeed, the report prepared by the Corporation of Delta points to a suspected regional change in operational or meteorological conditions as the cause of the decrease in dustfall.

The size distribution of the dustfall samples was also determined as part of this study (Table 3.13). For all the sampling periods, it appears that the mass distribution is overwhelmingly dominated by particles larger than 10 microns in diameter. Given that the large proportion of the sample being coal particles, this suggests that the coal dust exists primarily in the coarse mode. As such, it is expected that any coal PM enhancement caused by a passing train would result in an increase at larger size ranges rather than smaller sizes.

Table 3.12: Corporation of Delta dustfall measurement results for 2014.

Month	**Total Dustfall** (mg/dm^2)	**Daily Dustfall** (mg/dm^2/day)	**Coal** %	**Daily Coal Dustfall** (mg/dm^2/day)
April 2014	206.60	6.89	90	6.20
July 2014	141.43	4.71	80	3.77
October 2014	19.79	0.66	75	0.49
January 2015	21.45	0.71	15	0.11

Table 3.13: Corporation of Delta dustfall size distribution data for 2014.

Month	**Total Dustfall** (mg)	> 1 **mm** (mg)	$> 10\mu$**m** (mg)	**Between 3 and 10** μ**m** (mg)	**Between 1 and 3** μ**m** (mg)
April 2014	374.7	0	371.0	3.3	0.4
July 2014	256.5	0	254.3	1.6	0.6
October 2014	35.9	0	35.5	0.3	0.1
January 2015	38.9	0	38.2	0.4	0.3

3.5 Spatial Decay of PM Signal

In order to attempt to isolate the effect of distance from the railway on PM concentration, the means for PM_{10} concentration were calculated for both sites. The 15 m site had a mean of 15.7 $\mu g/m^3$, compared to a mean of 13.9 $\mu g/m^3$ at the 50 m site. Furthermore, the mean difference in concentration between the two sites was 2.04 $\mu g/m^3$. The variability of the measurements can be examined by calculating the standard deviation for each site. Once again, the 15 m site has a higher standard deviation (11.2 $\mu g/m^3$) than the 50 m site (9.72 $\mu g/m^3$), suggesting that the 15 m data includes more instances of extreme concentrations. This lends support to the idea that acute, short-term PM events such as a train passage or heavy traffic may affect the closer site more strongly. While this appears to be a small difference, these values were calculated using six weeks worth of data at a 1 minute resolution (nearly 60 000 data points).

When the PM data is stratified by wind direction, the 15 m site has a mean concentration of 16.21 $\mu g/m^3$ when the instruments are downwind of the highway and railway, compared to 14.52 $\mu g/m^3$ during upwind conditions (Figure 3.18). The 50 m site exhibits a similar trend (14.09 $\mu g/m^3$ for the downwind situation, 13.53 $\mu g/m^3$ for the upwind situation). Since the primary sources of PM_{10} in the area are the railway and highway, the impact of these sources would naturally decrease with distance, including any differences caused by wind direction. The variability of the upwind group at 15 m is also higher than that of the downwind group at 15 m (11.5 $\mu g/m^3$ vs. 10.4 $\mu g/m^3$). The differences between the two sites also exhibit some dependency on wind direction. Downwind conditions result in a larger difference between observations (2.41 $\mu g/m^3$) than upwind conditions (1.50 $\mu g/m^3$).

The PM data at the two sites can be stratified by train type (Figure 3.19), once again showing the elevated PM concentrations associated with coal trains compared to all trains, or control data. In addition, Figure 3.19 also shows the decrease in concentrations between the two distances. If the basic statistics for each group are examined (Table 3.14), the 50 m site has lower mean concentrations for all groups compared to the 15 m site. The magnitude of this decrease is approximately 1.0-2.0 $\mu g/m^3$ over the 35 m change in distance, and appears to be fairly consistent in terms of magnitude over the three groups. The change in variability also exhibits similar consistency across groups, including the control data.

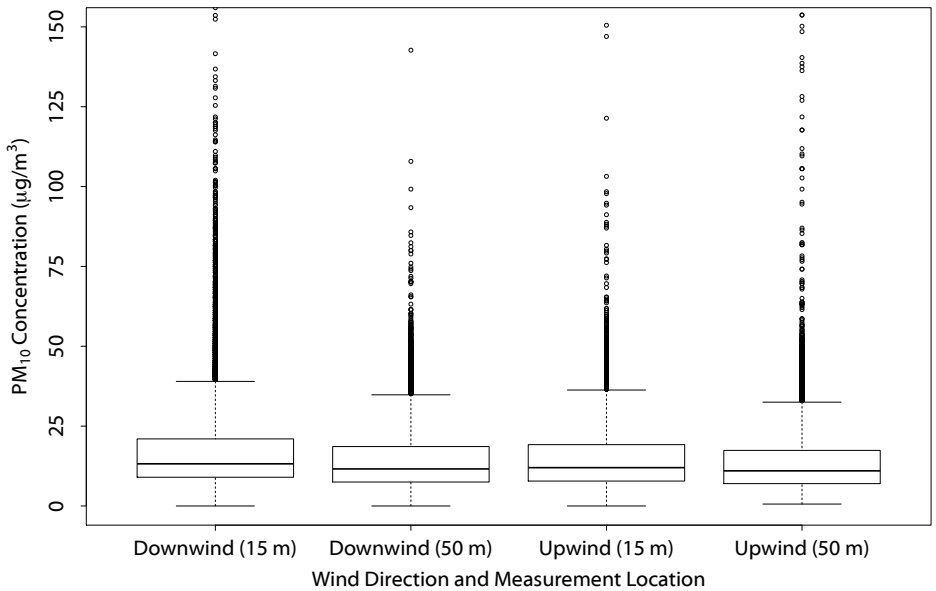

Figure 3.18: Comparison of PM_{10} measurements at two distances, stratified by wind direction. E-Sampler data.

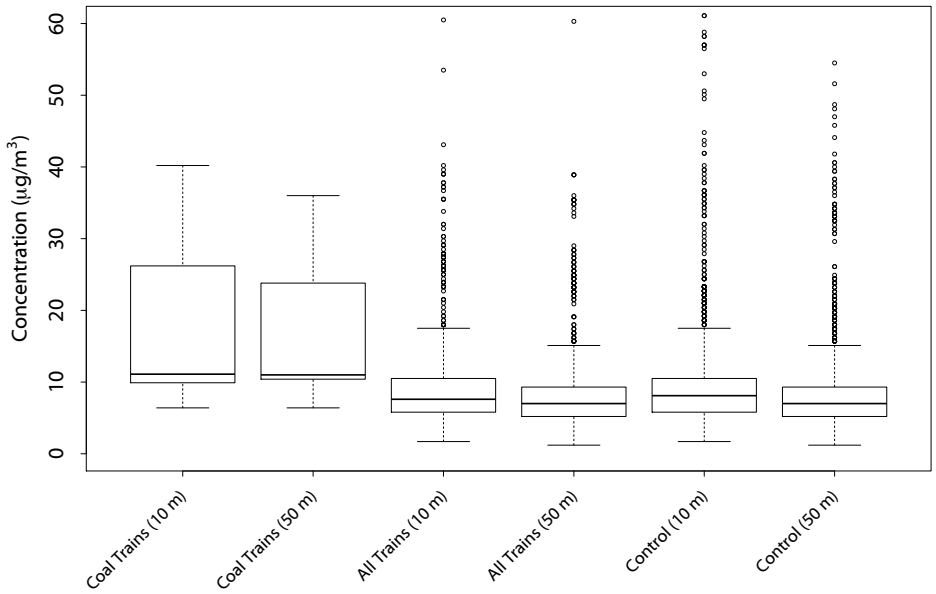

Figure 3.19: Comparison of PM_{10} measurements at two distances, stratified by train type. E-Sampler data.

Table 3.14: Basic statistics of PM concentrations at two distances, stratified by train type. E-Sampler data.

Group	**Mean** (g/m^3)	**Median** (g/m^3)	**Standard Deviation** (g/m^3)
		Coal Trains	
15 m	18.32	11.6	11.2
50 m	17.00	15.4	8.88
% Change	-7.24	+32.8	-20.7
		All Trains	
15 m	13.83	11.4	10.17
50 m	12.07	10.4	7.75
% Change	-12.8	-8.78	-23.8
		Control	
15 m	13.78	11.4	9.99
50 m	11.81	9.9	7.30
% Change	-14.3	-13.2	-27.0

3.6 Discussion

3.6.1 PM Enhancement Due to Trains (All Types)

When examining the overall impact that passing trains have on local PM concentration, there does not appear to be any significant relationship. It can be argued that this is in general agreement with studies such as Gehrig et al. (2007), that have found "small, however, measureable increases in ambient PM_{10} concentrations in the immediate vicinity of the tracks". The same study determined an "railway-induced" enhancement of PM_{10} concentration of between 1.4-2.0 $\mu g/m^3$. According to Table 3.2, the raw enhancement of PM concentration due to train passages is even smaller than these values, ranging from 0.26-0.44 $\mu g/m^3$ across the three size ranges analyzed in this study.

Interestingly, Gehrig et al. (2007)'s study took place in Switzerland, where virtually all train traffic is electric, suggesting that all PM emissions due to trains are non-exhaust in nature. However, there is some evidence of sharp increases in PM concentration during certain train passages in this study (discussed more in Chapter 4). Therefore, the overall lack of a large enhancement in PM concentration due to train passages in this study then suggests several hypotheses that will be discussed here. The potential PM enhancement due to trains may be masked by:

1. The proximity of a major highway to the study site, and its assumed temporal variability in emissions

2. Differing wind speed and directions that may serve to underestimate any potential enhancement

3. The zone of influence of the railway being relatively small

For this study, any emissions from the highway were considered part of the "background" PM present at the site. As the magnitude of emissions from the highway is ostensibly variable (due to varying traffic counts as per Figure 3.1), the background PM concentration will be affected by this variability (in addition to diurnal variability driven by meteorology). Therefore, any potential enhancement due to a passing train may be masked by variations in highway traffic at that specific time.

The local wind meteorology at this site, and the contrast between daytime and nightime conditions (Table 3.1) may also underestimate the effect of a passing train.

As train passages are relatively short-lived, any potential PM enhancement is highly dependent on the wind speed and wind direction at that exact time. Moreover, due to the prevailing wind directions after sunset, any enhancement caused by a passing train at night are less likely to be directly observed by the instruments (as in Section 4.1.3). Nevertheless, when the data is stratified by wind direction (Figure 3.10), there still do not appear to be significant enhancements caused by passing trains.

The background concentration of this site (including the effects of the highway) is however still elevated when compared to PM concentration data recorded by Metro Vancouver at a site not adjacent to a highway. The mean 24-hour $PM_{2.5}$ concentration at the Tsawwassen, BC (approximately 15 km southwest of John Oliver Park) for the same study period was recorded to be 5.7 $\mu g/m^3$. In comparison, the mean 24-hour PM_3 concentration at John Oliver Park during the study period was 11.97 $\mu g/m^3$. Due to the lack of a statistically significant PM increase due to passing trains, it appears that the difference between these two sites is primarily driven by the proximity of the highway.

3.6.2 PM Enhancement Due to Coal Trains

When a distinction is made between the type of train passing the site, coal trains are associated with a statistically significant increase in PM_3 and PM_{10} concentration (Tables 3.6-3.7). However, it must be noted that for PM_3 and PM_{20}, only seven coal trains were used in these analyses compared to 16 in the PM_{10} analysis due to unreliable data. Despite the overall significant PM increase associated with coal trains, the results in Chapter 4 show that not all coal trains exhibit an obvious PM concentration increase.

Interestingly, the increase in PM concentration associated with a passing coal train differs between size ranges. The mean PM_3 concentration during coal train passages is 53.8% higher than the control group, compared to a 33.3% increase in PM_{10} concentration, and a 17.0% increase in PM_{20} concentration. It should also be noted that the median concentration during coal train passages increased across all of PM_3, PM_{10}, and PM_{20} (50.6%, 16.9%, and 22.9%, respectively). If we consider PM_{20} to represent total suspended particulates (TSP), the proportion that each size range represents can be calculated. For the control data, PM_3 represents 65.5% of TSP, compared to 86.1% for the coal train data. PM_{10} represents 82.3% and 93.8% of TSP for control and coal train data, respectively. The larger increase in proportion of TSP for PM_3 seems to suggest that the PM enhancement associated with coal

trains is driven by smaller particles. The insignificant results in the PM_{20} post-hoc tests also support this conclusion (Table 3.8). This appears to be in contrast with the findings of Jaffe et al. (2014), which showed that the strongest PM concentration increases occurrred in larger size ranges. There is also strong evidence from the Corporation of Delta's dustfall measurements to support the claim that these larger particles are indeed coal particles (Table 3.13). One possible explanation for this is that Jaffe et al. (2014) had equipment set up closer to the railway than this study. Due to the larger distance involved, it is possible that more of the larger particles were able to settle out before reaching the instrumentation at John Oliver Park. This hypothesis will be explored in Section 3.6.3.

Another study on coal trains conducted in Australia (Higginbotham et al., 2013) had data showing extreme increases in PM concentration with coal train passages (up to a 13 fold increase in some cases). Nevertheless, variability was found in the measurements from the study, as 20% of passing coal trains did not produce any "discernible signature" (Higginbotham et al., 2013). The average PM concentration increase for the Australian study were found to be around 25 $\mu g/m^3$, much larger than the increases recorded at John Oliver Park. It is possible that the coal-carrying trains in Australia have different regulations regarding chemical treatments to reduce dust, but details on these regulations are unknown.

The results in Table 3.11 also show that there is an enhancement of PM_{10} concentration associated with coal trains during both downwind and upwind conditions. It is interesting that upwind conditions still result in an enhancement that is statistically significant, given the strong dependency of PM concentration on wind direction that has been discussed.

3.6.3 Zone of Influence

Determining a zone of influence for the highway and railway at John Oliver Park is quite challenging due to the numerous potential confounding factors. Previous studies such as Roorda-Knape et al. (1998) have examined how various pollutants are related to distance from a linear source such as a highway. Roorda-Knape et al. (1998) show evidence to suggest that concentrations of pollutants such as black smoke and NO_2 decrease with distance from a highway, but the results for $PM_{2.5}$ and PM_{10} are less clear. In addition, the importance of wind direction and the curvilinear relationship of pollutant concentration with distance was highlighted (Roorda-Knape et al., 1998).

In 2010, Karner et al. (2010) presented results that summarized 41 different studies looking at a variety of pollutants. Once again, the results for $PM_{2.5}$ and PM_{10} show evidence of a very gradual decay over distance, and even no trend at all in some cases (Karner et al., 2010). For the data showing gradual decay of PM_{10}, concentrations were found to reach background levels after 176 m (Karner et al., 2010). This would seem to suggest that the zone of influence for the linear sources at John Oliver Park extends past the 50 m site.

The key difference with this study compared to previous work on spatial relationships of pollutants is the burst-like nature of passing trains. While PM concentration trends from a continuously emitting line source such as a highway appear to gradually rise and fall, the enhancement that can be seen with an individual passing train can be very spiky in nature. The variability in PM concentration associated with these bursts of emission appears to sharply decrease over a short distance, as evidenced by the decrease of standard deviation with distance for coal trains and all trains groups (Table 3.14). During times without these bursts (the control data), variability also sharply decreases in the same manner with distance. Based on the data from this study, as well as previous work, the presence of the railway appears to have some measurable effect on PM concentration at distances over 50 m, but the extreme values caused by train passages are unlikely to be seen at further distances.

Chapter 4

Case Studies Using Mini-MPL Imagery

In this chapter, three intensive observation days are presented in order to:

1. Demonstrate the novel deployment of a mini micropulse lidar system for investigation of plumes from linear sources
2. Show detailed, high temporal resolution "signatures" of trains passages in cases where the train characteristics are well defined.

As such, this chapter provides a natural extension to the broad statistical analysis presented in Chapter 3, and illustrates the short time scales and day-to-day variability associated with the train passages.

4.1 Case Studies

4.1.1 August 14, 2014

The Mini-MPL was deployed from 11:03 until 20:36 local time on this day. During this time, six trains passed by the site. Three of these trains were coal trains, one of which was a loaded train traveling westbound.

From the PM data recorded by the GRIMM (Figure 4.2b), there appear to be strong increases in particulate matter associated with 4 of the 6 train passages across all size intervals. Interestingly, two of these trains were mixed freight trains, while

the other two were coal trains. If the wind plots for the same time period are examined (Figure 4.3), there does not appear to be any readily apparent trend explaining why only some of the trains were associated with an obvious increase in PM concentration. The lidar imagery from the same day (Figure 4.2a) shows the backscatter ratio through a horizontal cross-section oriented approximately southeast. From the imagery, there appears to be a consistent band of elevated backscatter that is persistent through the day, located at approximately 600 m. This band represents BC Highway 99, with the emissions from vehicular traffic increasing the amount of backscatter recorded by the MPL. The instrument also happened to be positioned at the height of the passing train cars, resulting in a blockage of the laser beam during most of the train passages. This is represented on the output as black bands that last for the approximate amount of time of a train passage ($\tilde{5}$-6 minutes).

During the train passages beginning at 14:52, 15:03, 17:30, 17:54, and 18:04 (Trains 1-5) there are short-term instances of elevated backscatter at distances close to the MPL. However, this elevated backscatter is not present during the train passage at 19:29. If the wind plot (Figure 4.3a) is examined once again, during the daytime the wind was coming from a generally southerly direction. Towards the later parts of the evening and sunset, the direction shifts more towards a southeasterly direction. This is confirmed by the along-railway component changing to a negative value around this time (Figure 4.3b). This could be a potential explanation as to why Train 6 at 19:29 is not associated with an increase in PM concentration from the GRIMM or MPL data.

Out of these six train passages, four of them are associated with a visible increase in PM concentration from the GRIMM data, within 5 minutes of the train passage (Figure 4.1). Interestingly, both freight trains (Trains 2 and 4) and coal trains (Trains 3 and 5) are associated with PM concentration increases. A summary of the PM data during all six passages is provided in Table 4.1. The most striking trend apparent here is that major increases in PM concentration occur within the 10-20 μm range, with the exception of Train 5. Train 5 is the only instance of a strong increase in concentration across all size ranges. Moreover, there does not appear to be a discernable difference on this day in terms of the effects of coal trains versus freight trains. Overall, either type of train may be associated with major increases of PM concentration, or little to no increases. Out of these six trains, Train 5 appears to be the most unique, with a strong PM concentration increase across all size ranges.

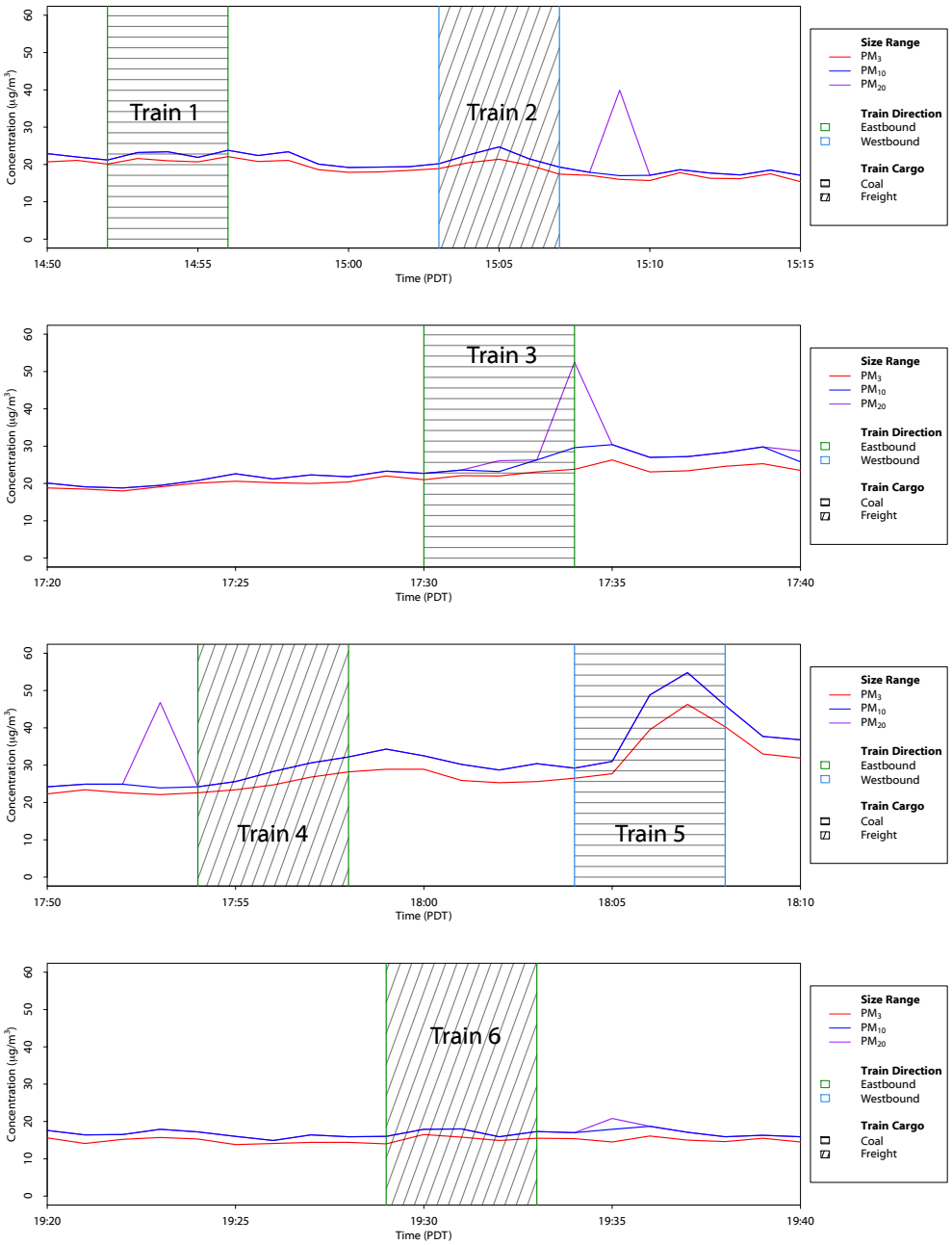

Figure 4.1: Individual train passages on August 14, 2014.

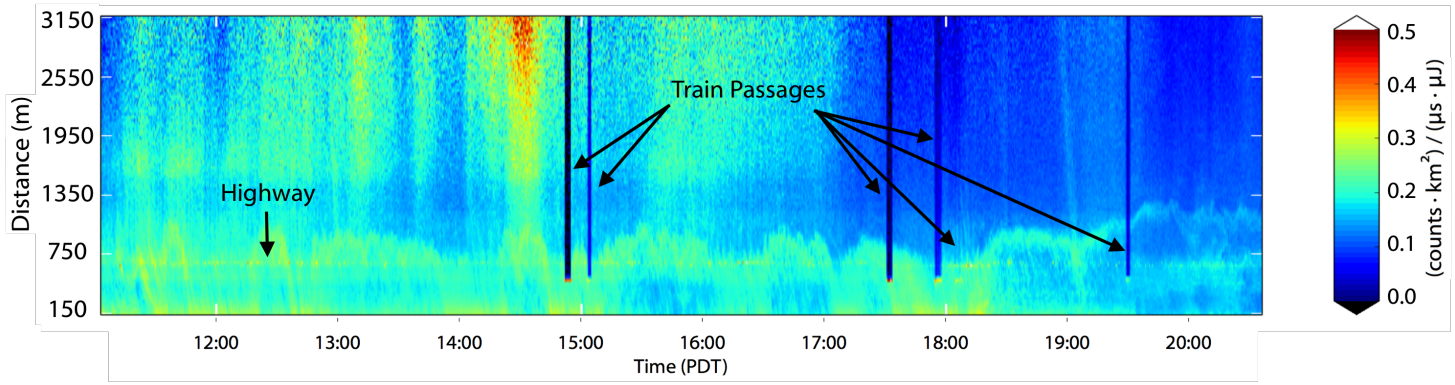

(a) Backscatter ratio

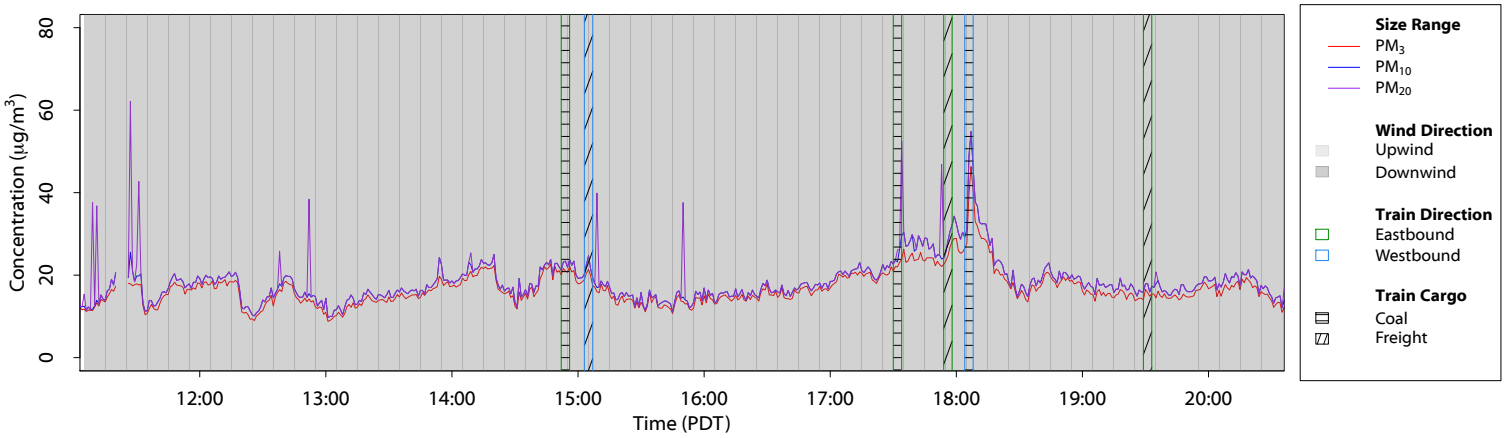

(b) PM concentration data

Figure 4.2: Lidar imagery and PM concentration for August 14, 2014. PM data recorded by GRIMM OPC.

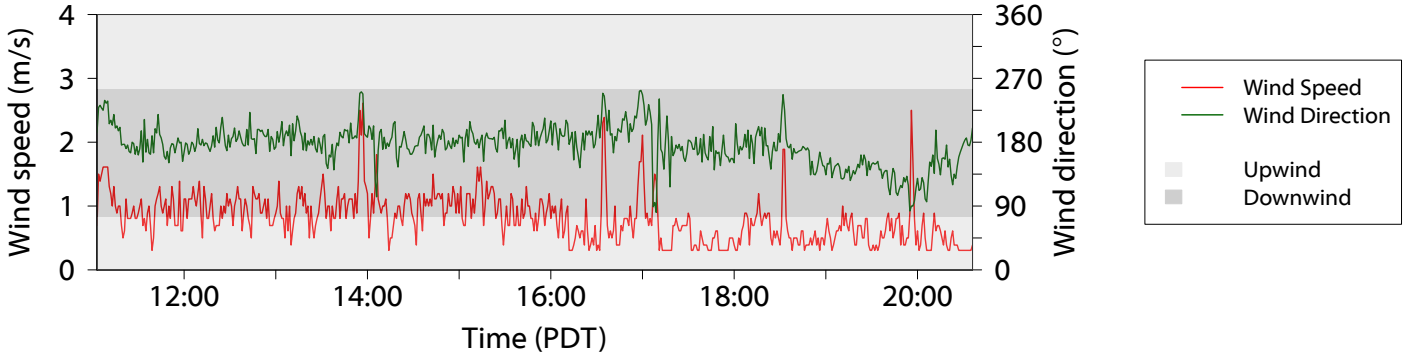

(a) Wind speed and direction

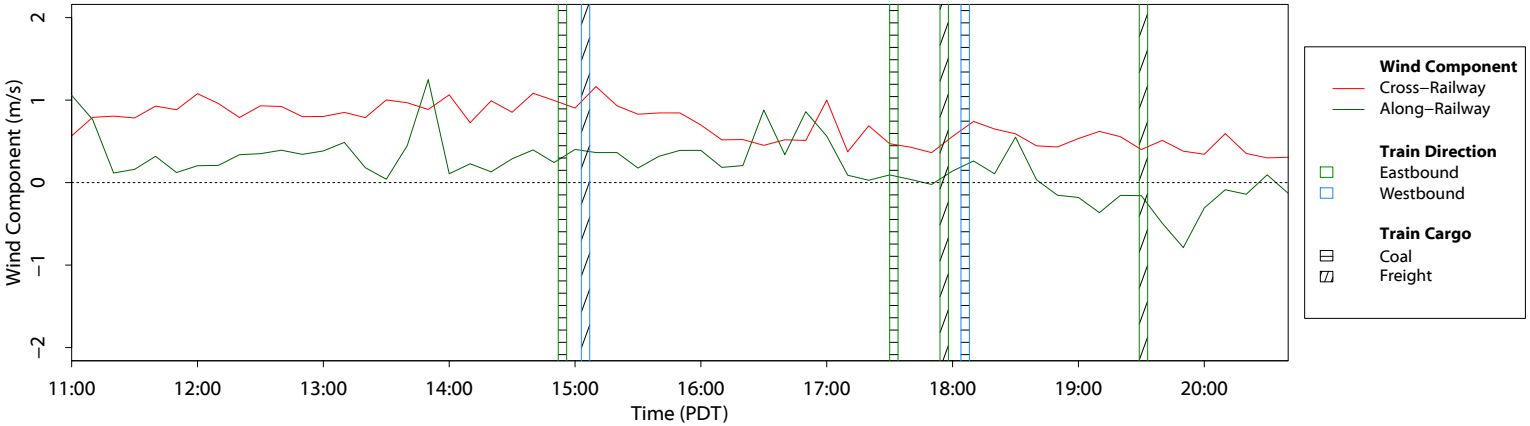

(b) Wind components

Figure 4.3: Wind direction and speed, and wind component plots for August 14, 2014. Recorded by Metro Vancouver.

Table 4.1: Summary of PM concentration data during train passages on August 14, 2014, recorded by GRIMM OPC.

Size Range	**Minimum** (g/m^3)	**Maximum** (g/m^3)	**% Increase**
Train 1 - Coal - 14:52 PDT			
PM_3	17.9	22.1	23.5
PM_{10}	19.2	23.8	24.0
PM_{20}	19.2	23.8	24.0
Train 2 - Freight - 15:03 PDT			
PM_3	15.7	21.4	36.3
PM_{10}	17.0	24.7	45.3
PM_{20}	17.1	39.9	133.3
Train 3 - Coal - 17:30 PDT			
PM_3	20.0	26.3	31.5
PM_{10}	21.2	30.4	43.4
PM_{20}	21.2	52.5	147.6
Train 4 - Freight - 17:54 PDT			
PM_3	22.1	28.9	30.8
PM_{10}	24.2	34.3	41.7
PM_{20}	24.2	46.8	93.4
Train 5 - Coal - 18:04 PDT			
PM_3	25.3	46.3	83.0
PM_{10}	28.7	54.8	90.9
PM_{20}	28.7	54.8	90.9
Train 6 - Freight - 19:29 PDT			
PM_3	13.8	16.5	19.6
PM_{10}	14.9	18.7	25.5
PM_{20}	14.9	20.8	40.0

4.1.2 August 26, 2014

The Mini-MPL was deployed from 08:50 until 17:30 PDT on this day. During this time, eight trains passed by the site. Four of these trains were coal trains, three were freight trains, and one was unidentified. The PM concentration data recorded by the GRIMM on this day was found to be unreliable, and due to this Metro Vancouver's data were used in the following analysis. The data recorded on this day represents very different conditions than August 14th. Firstly, only one of the train passages (occurring at approximately 16:00) appears to be directly associated with an increase in PM concentration. Moreover, this train passage is a freight train, rather than a coal train. There does appear to be a spike in PM concentration shortly before the coal train passage at 16:47 (Train 7), but it is unclear whether this spike is due to the train passages. Another spike in concentration occurs in the morning, around 9:40 AM, which appears to be well separated from any train passages. In general, the background trend in PM concentration seems to agree with the results discussed in Section 3.1.1, where concentration decreases during the afternoon after the morning rush hour, and slowly rises to coincide with the afternoon rush hour.

If the lidar imagery is examined (Figure 4.5a), there is once again a sharp contrast to the imagery taken on August 14. Firstly, there appears to be a second persistent band of elevated backscatter ratio occurring at approximately 1600 m. Since lidar returns at this distance begin to become unreliable due to the optical thickness of the layer, it is unclear what is causing this feature. During the morning hours, backscatter appears to be elevated, being in agreement with the higher observed PM concentrations. During the afternoon, the MPL records a markedly clearer cross-section, again agreeing with the PM data that shows relatively lower concentrations that are consistent and steady. The large increase in PM concentration associated with the train passage at 16:00 (Figure 4.4) is also visible in the MPL data as a visible plume that appears to move towards the MPL.

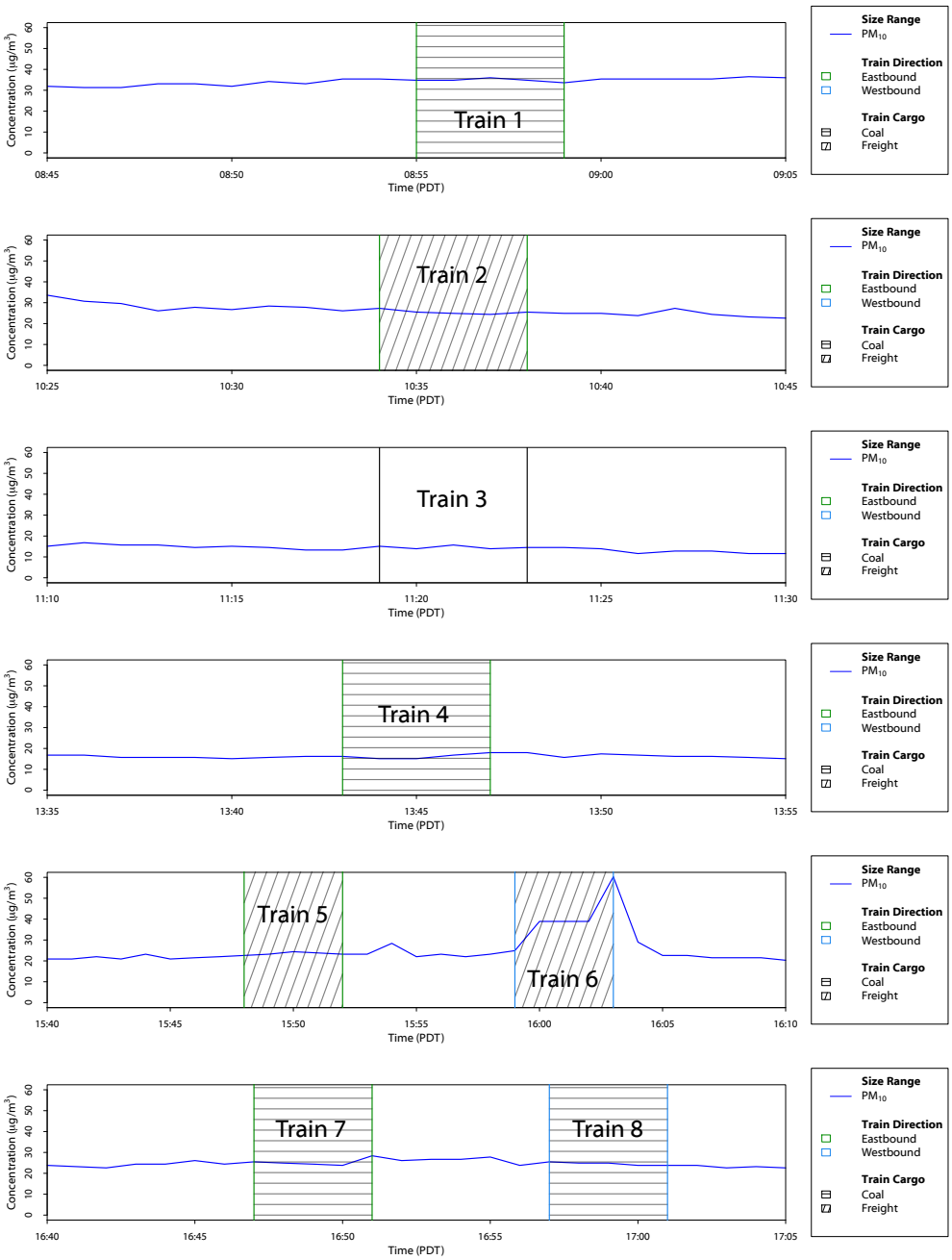

Figure 4.4: Individual train passages on August 26, 2014.

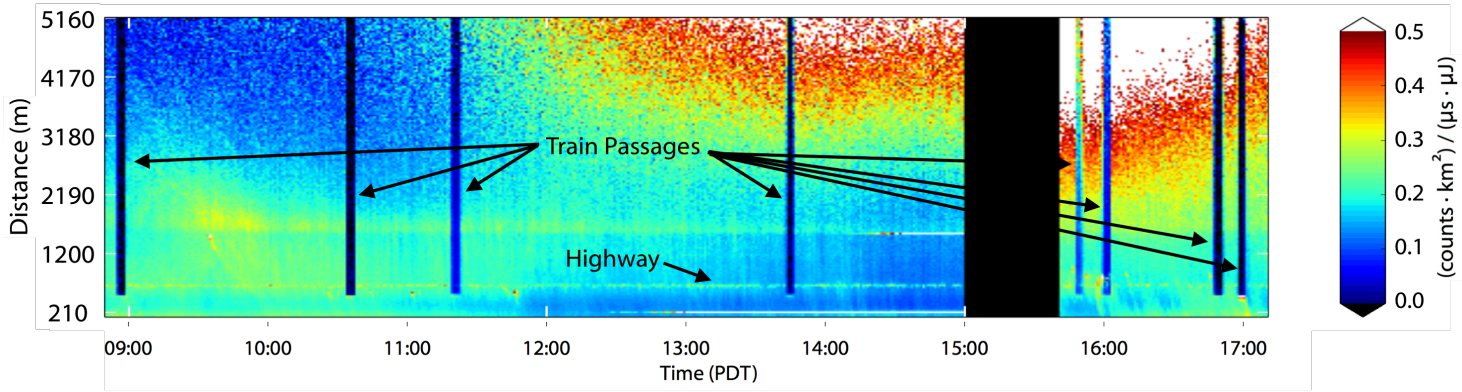

(a) Backscatter ratio

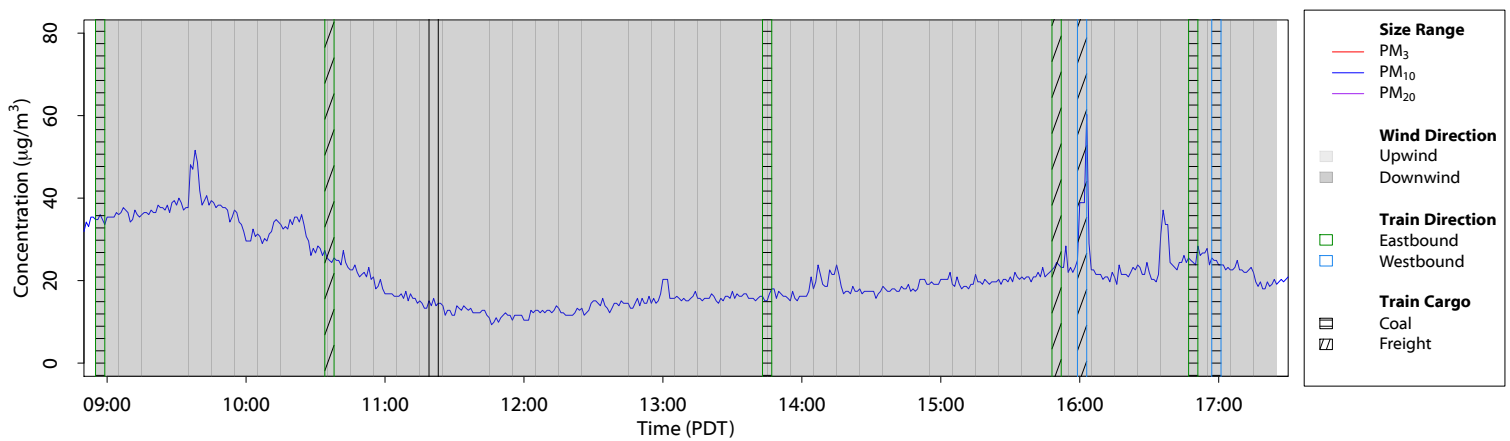

(b) PM concentration data

Figure 4.5: Lidar imagery and PM concentration for August 26, 2014, recorded by E-Sampler.

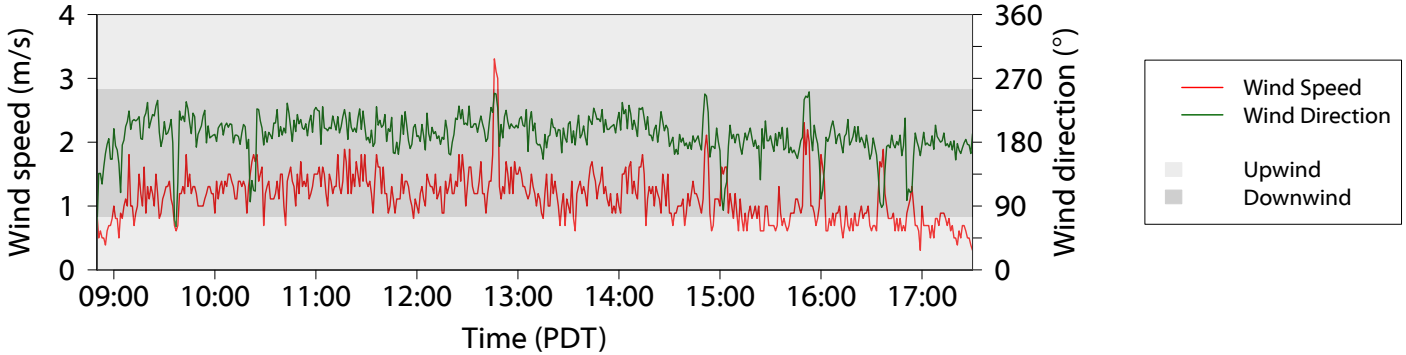

(a) Wind speed and direction

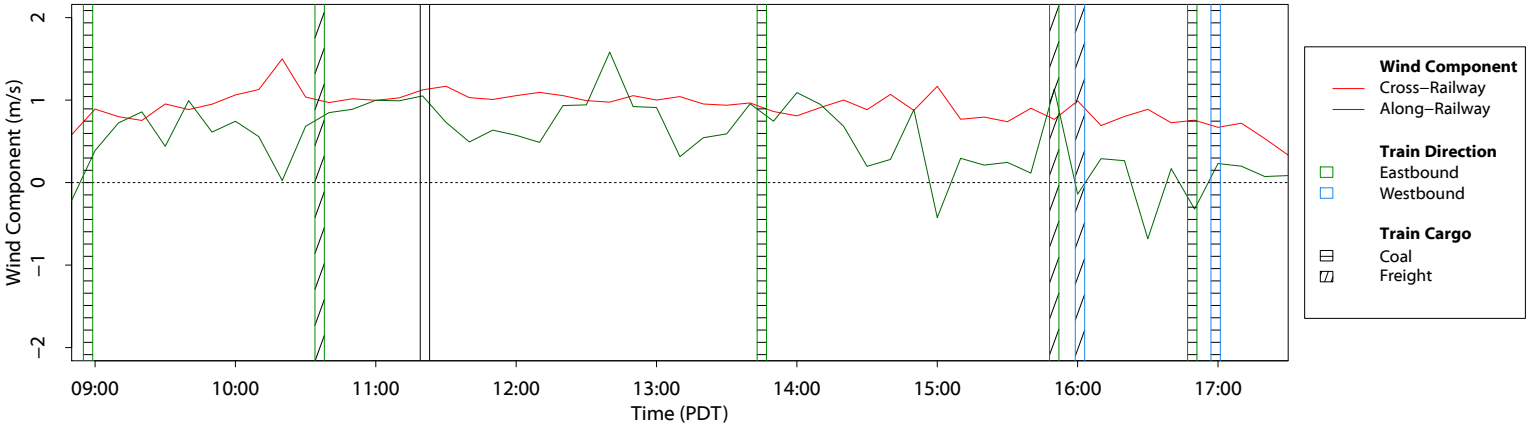

(b) Wind components

Figure 4.6: Wind direction and speed, and wind component plots for August 26, 2014. Recorded by Metro Vancouver.

4.1.3 September 4, 2014

The Mini-MPL was deployed from 13:04 until 21:39 PDT on this day. During this time, six trains passed by the site. Three of these trains were coal trains, one of which was a loaded train traveling westbound. The wind conditions on this day are quite different than the previous two examples that have been discussed. First and foremost, the wind is predominantly northwesterly for most of the day (Figure 4.6a), a sharp contrast to the southerly conditions that dominate the other two days discussed. As such, the cross-railway wind component is negative for the majority of the day (until a reversal at sunset), signifying that the wind is blowing away from the instruments (Figure 4.9b). Due to this, observed PM concentrations should be lower than when the cross-railway wind component is positive, since the major source of PM (the highway) would be generating a plume that moves away from the instruments. The PM data in Figure 4.8b reflects this, with lower concentrations compared to August 14 and 26, and very few instances of short-term spikes in concentration. The results from this day lend support to the dominating influence of wind direction on PM concentration.

In comparison to August 14 and 26, the MPL data also appears to show a relatively clean atmosphere through the day. There does appear to be some elevated backscatter at a distance slightly beyond the highway that is persistent through most of the day. However, it does not appear that this feature is associated with any road or rail traffic. The only instance of a PM increase caused by a train passage being picked up by the MPL is at 20:41 (Train 6). This freight train passage coincides with the MPL imagery showing a plume being generated. This plume, emanating at the time and distance associated with the train passage appears to move away from the MPL, which is consistent with the wind data at that time (Figure 4.9).

The GRIMM data during each train passage (Figure 4.7) confirms that no train passage is associated with an enhancement of PM, except for Train 6. Interestingly, there appear to be two peaks in concentration, one just before the train passes, and one approximately 5 minutes after the passage. If the lidar imagery is examined once again during that time (Figure 4.8a), there appear to be strong sources of PM that are at distances other than the railway or highway. It is unknown what these sources could be, but given the change in wind direction, the GRIMM may be recording the effect of these sources at that time.

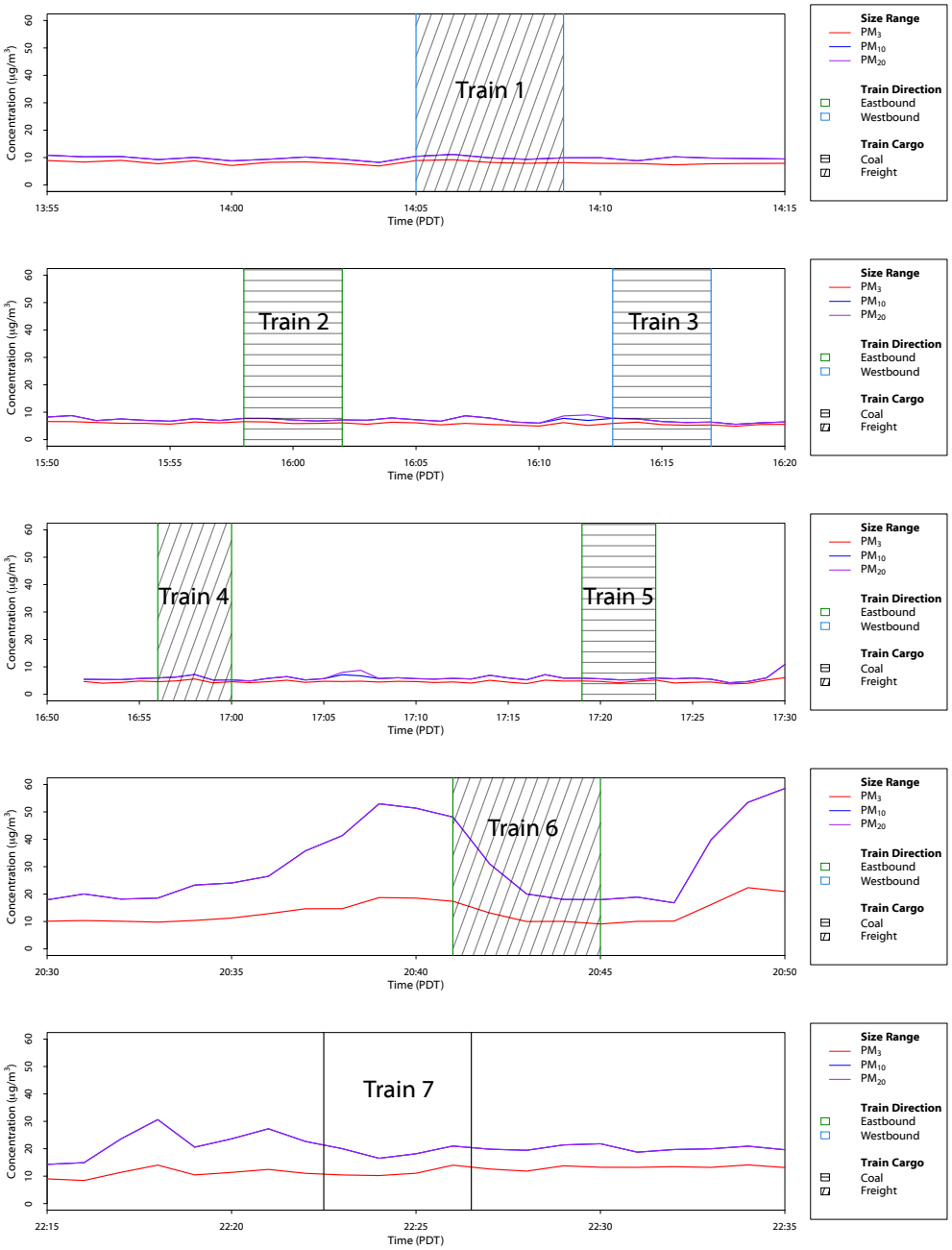

Figure 4.7: Individual train passages on September 4, 2014.

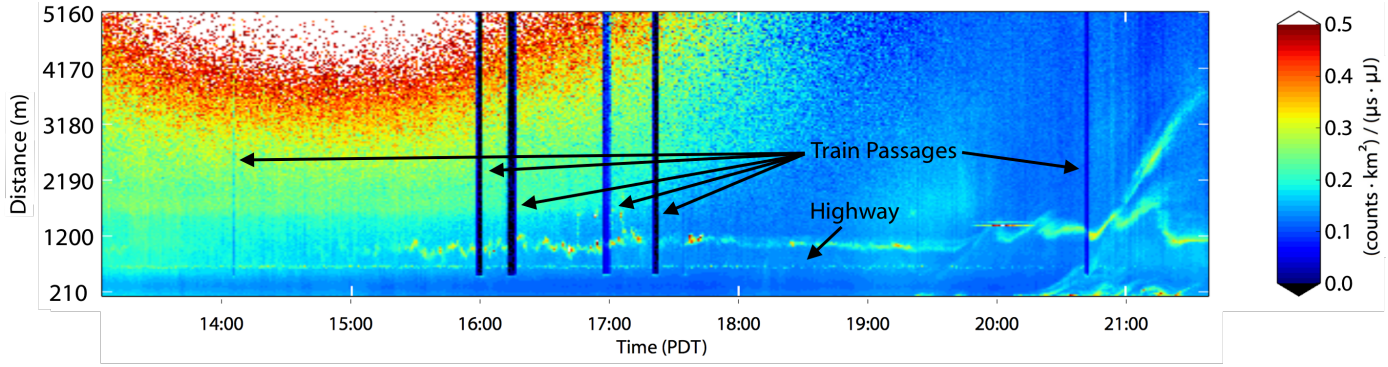

(a) Backscatter ratio

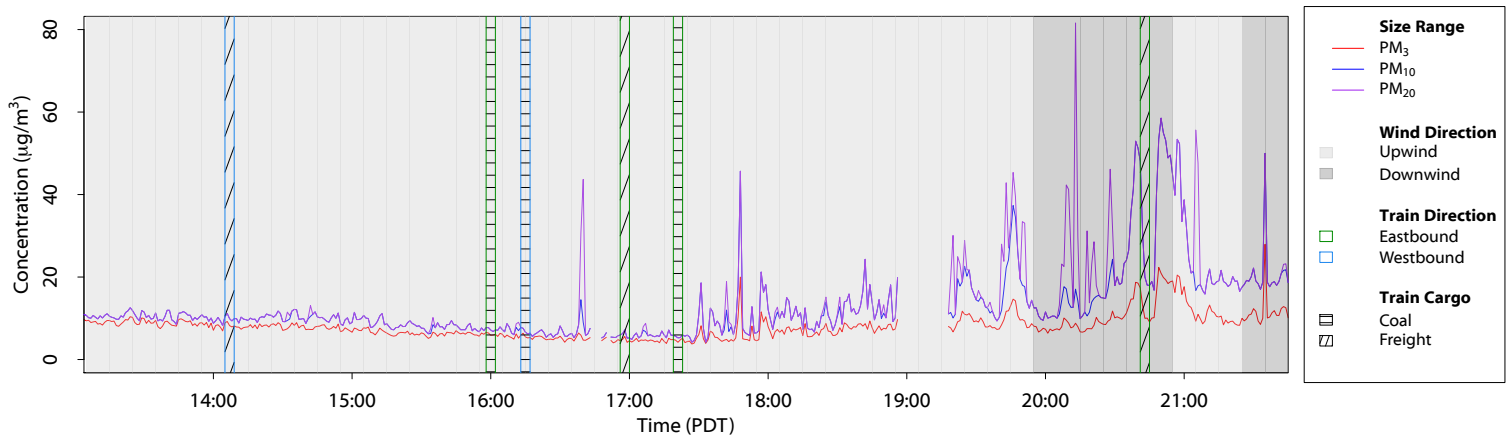

(b) PM concentration data

Figure 4.8: Lidar imagery and PM concentration for September 4, 2014, recorded by GRIMM OPC.

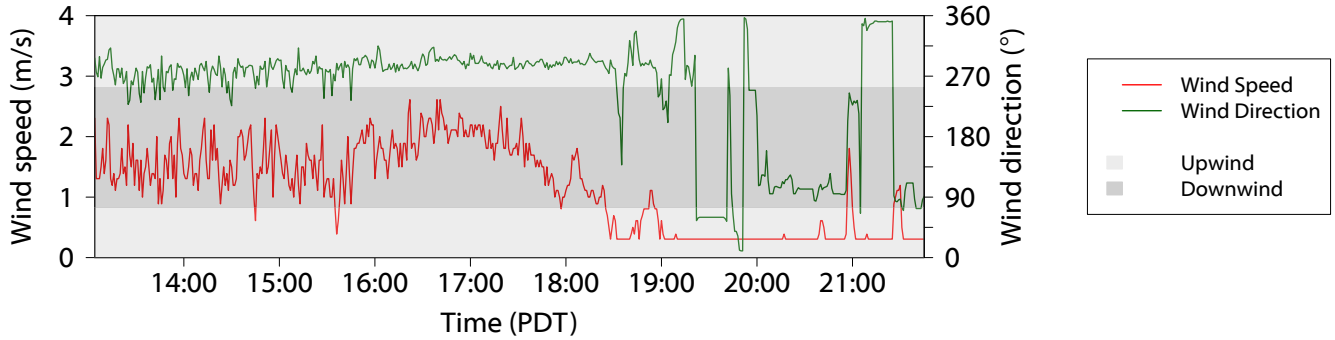

(a) Wind speed and direction

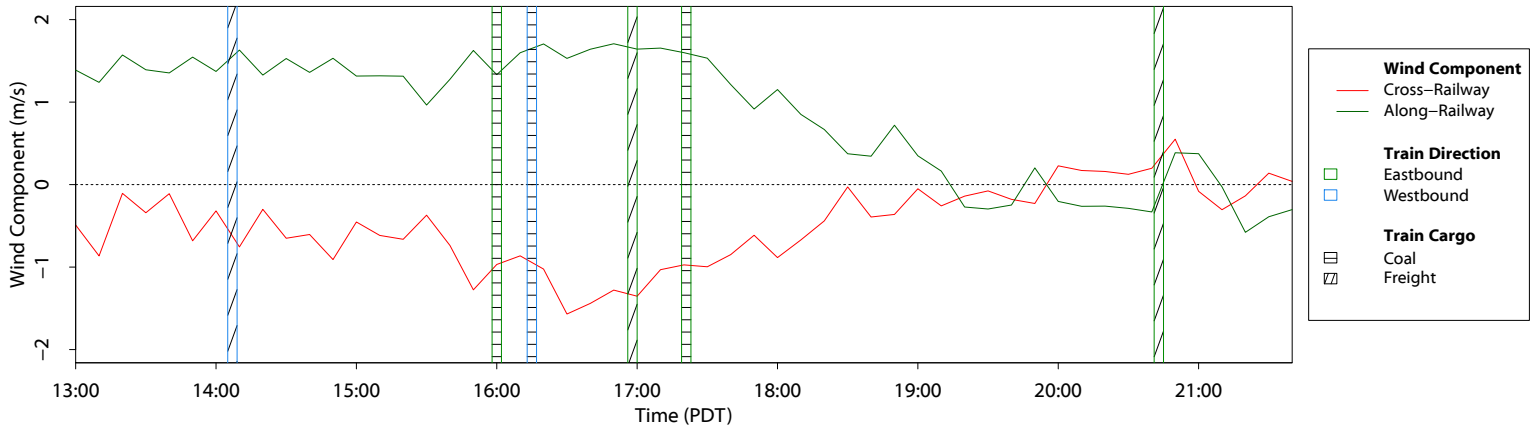

(b) Wind components

Figure 4.9: Wind direction and speed, and wind component plots for September 4, 2014. Recorded by Metro Vancouver.

Table 4.2: Summary of PM concentration data during train passages on September 4, 2014, recorded by GRIMM OPC.

Size Range	**Minimum** (g/m^3)	**Maximum** (g/m^3)	**% Increase**
	Train 1 - Freight - 14:05 PDT		
PM_{10}	8.24	11.2	35.3
	Train 2 - Coal - 15:58 PDT		
PM_{10}	6.72	8.70	29.5
	Train 3 - Coal - 16:13 PDT		
PM_{10}	5.58	7.78	39.4
	Train 4 - Freight - 16:56 PDT		
PM_{10}	4.85	7.20	48.5
	Train 5 - Coal - 17:19 PDT		
PM_{10}	4.20	7.16	70.5
	Train 6 - Freight - 20:41 PDT		
PM_{10}	16.8	58.5	248.2
	Train 7 - Unknown - 22:22 PDT		
PM_{10}	16.5	30.6	85.5

4.2 Discussion

Examining a series of individual train passages helps to determine the range of possible outcomes associated with a passing train. There are certainly instances of sharp increases in PM concentration with a passing coal train, but there are also increases associated with passing freight trains. From the data presented here, it is clear that the passage of a train is not guaranteed to result in an increase of PM concentration. However, when a PM increase occurs, it does tend to be across both fine and coarse modes. A potential explanation for this relates back to the three potential sources of PM associated with a train passage. According to previous work (Abbasi et al., 2013; Jaffe et al., 2014), PM can be generated by a passing train through various processes:

- the diesel locomotive itself
- particles formed from the wearing down of rails and other materials
- particles on the ground introduced into the air due to the turbulence caused by the passing train
- in the case of coal-carrying trains, coal dust lost into the air from the open cars

It is difficult to discriminate between these sources without chemical analysis (which was not performed as part of this study), but there are various indicators that suggest what processes are at work. Size segregated measurements can help discern between the various sources. In previous studies, 90% of DPM was shown to be smaller than 1.0 μm in diameter (Liukonen et al., 2002), suggesting that a strong increase in concentration at larger size ranges would not be due to DPM. Since the results show an increase across all size ranges, it appears that more than just DPM is contributing to the PM enhancement during train passages. Moreover, the results of the dustfall study showing the presence of coal particles in the collected samples shows the influence of coal-carrying trains as a PM source. The PM enhancement during some freight train passages serves as evidence of the non-exhaust sources (wearing down of materials, and ground particles) also being present. As some freight trains are associated with an increase in PM across all size ranges, the coarse mode particles would likely be generated from a combination of these two sources (Abbasi et al., 2013). As the largest concentration increase during a coal train

passage occurs with PM_3 (Section 3.6.2), it would appear that the instruments set up at 50 m were most affected by the smaller particles associated with DPM, rather than the other non-exhaust sources.

There is some evidence that wind direction is the most important factor in determining if an enhancement will be seen at a certain location beside a linear source. The data for September 4, 2014 shows that none of the train passages during the day are associated with an increase in PM. The wind direction at this time showed a negative cross-railway component, indicating upwind conditions. However, the reversal of wind direction at night appears to drive the increase in PM concentration associated with the train passage at 20:41 PDT. The wind speed during all of the days examined in this chapter was relatively low (typically between 1-2 m/s), suggesting a small degree of mixing of pollutants in the atmosphere. Due to this, plume movement may not be as pronounced as in other situations. In complex coastal terrain, any effect of pollutant sources will be strongly dependent on phenomena such as land/sea breeze circulations.

The mini-MPL served as a useful tool in examining plume movement, as well as confirming some of the OPC data. The plumes that are visible in the lidar imagery demonstrate the various sources that are present at the site, indicating its utility in the qualitative examination of a site's sources and sinks. However, given the short range of the mini-MPL when operated horizontally, there are certain drawbacks associated with its usage.

Moreover, the analysis of this data from a case study perspective illustrates the trends and patterns that are not identified by general statistical tests. The results of these case studies show that the issue of PM enhancement is quite complex, and requires large amounts of data and a coordinated data collection plan.

Chapter 5

Conclusions

5.1 Key Findings

The statistical analyses performed in Chapter 3 yielded several key conclusions:

- The increase in PM concentration associated with a train passage of any type is modest and highly variable (average increases of 0.21, 0.44, and 0.23 μg/m^3 were found for PM_3, PM_{10}, and PM_{20}, respectively)
- Observed PM concentration is highly dependent on wind direction. Downwind conditions are associated with higher PM concentrations than upwind conditions. For control condtions, the mean enhancement due to wind direction is 2.35, 1.61, and 1.70 μg/m^3 for PM_3, PM_{10}, and PM_{20}, respectively
- Coal trains were associated with a statistically significant ($\alpha = 0.01$) PM concentration increase of 53.8%, 33.3%, and 17.0% for PM_3, PM_{10}, and PM_{20}, respectively, at a distance of 50 metres from the tracks
- PM_3 represented 65.5% of total suspended particulates (TSP) during control conditions, compared to 86.1% during coal train passages. PM_{10} represented 82.3% of TSP during control conditions, and 93.8% of TSP during coal train passages
- Train passages have an identifiable effect on PM concentrations at both the 15 m and 50 m sites

- The variability of PM concentrations during train passages sharply decreases with distance

When the lidar data was analyzed in conjunction with high temporal resolution PM concentration and wind data, the results expand on the conclusions from Chapter 4. The high resolution data shows:

- A PM concentration enhancement was not present for all observed train passages
- When a PM concentration enhancement was observed, it tended to be present across all measured size ranges
- There is evidence of PM concentration enhancements being present with both freight and coal train passages
- In some instances, plumes generated from a train passage could be seen on the backscatter output
- Wind direction strongly influences observed PM concentrations, as evidenced by the results from September 4, 2014 (Section 4.1.3)
- There is evidence to suggest the presence of both exhaust (DPM), and non-exhaust sources (wearing down of railway materials, ground-level particles being disturbed by turbulence, and coal dust from coal-carrying trains)

Overall, the usage of a variety of data sources in addition to wind data is crucial in determining the presence of a PM enhancement effect due to passing trains. Statistical analysis of a sufficiently large data set is useful in quantifying any effects from passing trains, but a more in-depth look at individual train passages provides conclusions that are helpful from a more practical standpoint. Due to the short-term nature of a train passage, it is unlikely that the enhancement effect due to passing trains would cause a violation of current PM standards, as these standards are measured on much longer time scales.

5.1.1 Study Limitations & Future Research

The results from this study present numerous interesting possibilities for future work. Firstly, the reliability problems surrounding some of the data recorded by the GRIMM may be resolved with a setup less sensitive to adverse weather conditions. Furthermore, due to the sharp decrease in variability between the 15 m and 50 m sites (Section 3.5), it is likely that placing the GRIMM closer to the railway would result in a higher sensitivity to any effect caused by the railway.

The results from Section 3.5 demonstrate an opportunity for more research to be conducted on the spatial decay of PM generated by a railway. The location used in this study was not optimal for investigating this, due to the influence of the highway nearby. More PM measurements at several distances from a railway would be helpful in characterizing the relationship between PM concentration and distance.

In addition, studies of this nature at a different site would be quite useful in examining how local meteorology processes govern any effects caused by a railway. Understanding the effects of local meteorology would serve to better predict the impact that rail traffic would have on any residents who happen to live in close proximity. The results from the Corporation of Delta dustfall study show that the amount of observed coal dust differs based on the time of year. More research on coal dust during the winter would be useful in exploring this phenomenon under a wider range of meteorological conditions. There has been previous evidence of certain coal trains that emit very large amounts of coal dust (Jaffe et al., 2014), but there is little knowledge on how to predict these events. Furthermore, the detection of strong PM concentration enhancements caused by coal trains may be due to the experimental set up used in this study. Particle loss within the Teflon tubing of the GRIMM caused by sedimentation and impaction may have underestimated PM concentrations, especially at larger particle sizes.

The limitations presented by the small sample size of the train passage data presented in this study could be rectified by a more robust methodology of train identification. Potential ways to achieve this include motion-activated cameras that can operate in night-time conditions, similar to those used in Jaffe et al. (2014). In addition, instrumentation that can measure a wider variety of pollutants such as CO_2 can serve to supplement the analysis of PM concentration. The nature of coal dust generation from trains is also somewhat unclear without more information on the chemical surfactants used by train companies to prevent coal dust from leaving

the cars. More detail on these processes would be highly useful in understanding the conditions under which coal dust is generated.

Bibliography

Abbasi, S., Jansson, A., Sellgren, U., and Olofsson, U. (2013). Particle Emissions From Rail Traffic: A Literature Review. *Critical Reviews in Environmental Science and Technology*, 43(23):2511–2544.

Abbasi, S., Olander, L., Larsson, C., Olofsson, U., Jansson, A., and Sellgren, U. (2012). A field test study of airborne wear particles from a running regional train. *Proceedings of the Institution of Mechanical Engineers Part F-Journal of Rail and Rapid Transit*, 226(F1):95–109.

Bascom, R., Bromberg, P. A., Costa, D. A., Devlin, R., Dockery, D. W., Frampton, M. W., Lambert, W., Samet, J. M., Speizer, F. E., and Utell, M. (1996). Health effects of outdoor air pollution. *American Journal of Respiratory and Critical Care Medicine*, 153(1):3–50.

Cascadia Discovery Institute (2011). Seattle, WA - Vancouver, BC Cross-border Freight Rail Improvement Study. Technical report.

Charron, A. and Harrison, R. M. (2005). Fine (PM2.5) and coarse (PM2.5-10) particulate matter on a heavily trafficked London highway: Sources and processes. *Environmental Science & Technology*, 39(20):7768–7776.

Corporation of Delta (2014a). Coal dustfall monitoring update. Technical Report F.16.

Corporation of Delta (2014b). Port Metro Vancouver project approval for Fraser Surrey Docks direct transfer coal facility. Technical Report F.03.

Corporation of Delta (2015). Coal dustfall monitoring update. Technical Report F.17.

Dockery, D. W. and Pope, C. A. (1994). Acute Respiratory Effects of Particulate air-Pollution. *Annual Review of Public Health*, 15:107–132.

Ferreira, A. D. and Vaz, P. A. (2004). Wind tunnel study of coal dust release from train wagons. *Journal of Wind Engineering and Industrial Aerodynamics*, 92(7-8):565–577.

Ferreira, A. D., Viegas, D. X., and Sousa, A. (2003). Full-scale measurements for evaluation of coal dust release from train wagons with two different shelter covers. *Journal of Wind Engineering and Industrial Aerodynamics*, 91(10):1271–1283.

Fridell, E., Ferm, M., and Ekberg, A. (2010). Emissions of particulate matters from railways - Emission factors and condition monitoring. *Transportation Research Part d-Transport and Environment*, 15(4):240–245.

Galvis, B., Bergin, M., and Russell, A. (2013). Fuel-based fine particulate and black carbon emission factors from a railyard area in Atlanta. *Journal of the Air & Waste Management Association*, 63(6):648–658.

Gehrig, R., Hill, M., Lienemann, P., Zwicky, C. N., Bukowiecki, N., Weingartner, E., Baltensperger, U., and Buchmann, B. (2007). Contribution of railway traffic to local PM10 concentrations in Switzerland. *Atmospheric Environment*, 41(5):923–933.

GRIMM Aerosol Technik GmbH & Co. KG (2010). *Portable Laser Aerosolspectrometer and Dust Monitor Model 1.108/1.109*.

Gustafsson, M., Blomqvist, G., Swietlicki, E., Dahl, A., and Gudmundsson, A. (2012). Inhalable railroad particles at ground level and subterranean stations - Physical and chemical properties and relation to train traffic. *Transportation Research Part d-Transport and Environment*, 17(3):277–285.

Hahn, I., Brixey, L. A., Wiener, R. W., Henkle, S. W., and Baldauf, R. (2009). Characterization of traffic-related PM concentration distribution and fluctuation patterns in near-highway urban residential street canyons. *Journal of Environmental Monitoring*, 11(12):2136–2145.

Hays, M. D., Cho, S.-H., Baldauf, R., Schauer, J. J., and Shaferd, M. (2011). Particle size distributions of metal and non-metal elements in an urban near-highway environment. *Atmospheric Environment*, 45(4):925–934.

Heyder, J. (2004). Deposition of Inhaled Particles in the Human Respiratory Tract and Consequences for Regional Targeting in Respiratory Drug Delivery. *Proc Am Thorac Soc*, 1:315–320.

Higginbotham, N., Ewald, B., Mozeley, F., and Whelan, J. (2013). Coal train pollution signature study. Technical report.

Hoek, G., Brunekreef, B., Goldbohm, S., Fischer, P., and van den Brandt, P. A. (2002). Association between mortality and indicators of traffic-related air pollution in the Netherlands: a cohort study. *LANCET*, 360(9341):1203–1209.

Jaffe, D. A., Hof, G., Malashanka, S., Putz, J., Thayer, J., Fry, J. L., Ayres, B., and Pierce, J. R. (2014). Diesel particulate matter emission factors and air quality implications from in-service rail in Washington State, USA. *Atmospheric Pollution Research*, 5(2):344–351.

Karner, A. A., Eisinger, D. S., and Niemeier, D. A. (2010). Near-Roadway Air Quality: Synthesizing the Findings from Real-World Data. *Environmental Science & Technology*, 44(14):5334–5344.

Kilburn, K. H. (2000). Effects of Diesel Exhaust on Neurobehavioral and Pulmonary Functions. *Archives of Environmental Health: An International Journal*, 55(1):11–17.

Liukonen, L. (2003). Diesel particulate matter exposure to railroad train crews - Authors' reply. *Aiha Journal*, 64(2):169–169.

Liukonen, L. R., Grogan, J. L., and Myers, W. (2002). Diesel particulate matter exposure to railroad train crews. *Aiha Journal*, 63(5):610–616.

Maletto, A., McKendry, I. G., and Strawbridge, K. B. (2003). Profiles of particulate matter size distributions using a balloon-borne lightweight aerosol spectrometer in the planetary boundary layer. *Atmospheric Environment*, 37(5):661–670.

McKendry, I. G. (2000). PM10 levels in the Lower Fraser Valley, British Columbia, Canada: An overview of spatiotemporal variations and meteorological controls. *Journal of the Air & Waste Management Association*, 50(3):443–452.

Merbitz, H., Fritz, S., and Schneider, C. (2012). Mobile measurements and regression modeling of the spatial particulate matter variability in an urban area. *Science of the Total Environment*, 438:389–403.

Peters, A., Wichmann, H. E., Tuch, T., Heinrich, J., and Heyder, J. (1997). Respiratory effects are associated with the number of ultrafine particles. *American Journal of Respiratory and Critical Care Medicine*, 155(4):1376–1383.

Peters, T. M., Ott, D., and O'Shaughnessy, P. T. (2006). Comparison of the grimm 1.108 and 1.109 portable aerosol spectrometer to the tsi 3321 aerodynamic particle sizer for dry particles. *Ann Occup Hyg*, 50(8):843–50.

Petrovic, V. (2008). Particulate matters from diesel engine exhaust emission. *Thermal Science*, 12(2):183–198.

Port Metro Vancouver (2014). Port Overview. Technical report.

Pronk, A., Coble, J., and Stewart, P. A. (2009). Occupational exposure to diesel engine exhaust: A literature review. *Journal of Exposure Science and Environmental Epidemiology*, 19(5):443–457.

Roorda-Knape, M. C., Janssen, N., de Hartog, J. J., van VLiet, P., Harssema, H., and Brunekreef, B. (1998). Air pollution from traffic in city districts near major motorways. *Atmospheric Environment*, 32(11):1921–1930.

Seinfeld, J. H. and Pandis, S. N. (2006). *Atmospheric Chemistry and Physics: From Air Pollution to Climate Change*. Wiley.

Statistics Canada (2014). Population and dwelling counts, for Canada, provinces and territories, and population centres, 2011 and 2006 censuses. Technical report.

Steyn, D. G., Bottenheim, J. W., and Thomson, R. B. (1997). Overview of tropospheric ozone in the Lower Fraser Valley, and the Pacific '93 Field Study. *Atmospheric Environment*, 31(14):2025–2035.

Stull, R. B. (1988). *An introduction to boundary layer meteorology*. Springer.

Thai, A., McKendry, I., and Brauer, M. (2008). Particulate matter exposure along designated bicycle routes in Vancouver, British Columbia. *Science of the Total Environment*, 405(1-3):26–35.

von der Weiden, S.-L., Drewnick, F., and Borrmann, S. (2009). Particle loss calculator - a new software tool for the assessment of the performance of aerosol inlet systems. *Atmospheric Measurement Techniques*, 2:479–494.

Welch, B. L. (1951). On the Comparison of Several Mean Values - an Alternative Approach. *Biometrika*, 38(3-4):330–336.

Westshore Terminals Ltd (2014). The Terminal. Technical report.

Zhu, J., Aikawa, B., and Pigeon, R. (2005). Measurement of Fine Particles in Diesel Emissions Using a Real-Time Aerosol Monitor. *Journal of the Air & Waste Management Association*, 55(7):978–983.

Zhu, Y. F., Hinds, W. C., Kim, S., Shen, S., and Sioutas, C. (2002). Study of ultrafine particles near a major highway with heavy-duty diesel traffic. *Atmospheric Environment*, 36(27):4323–4335.